Table 1 CSR and SHM activity of mutant human AID relative to wild-type human and mouse AID

Group	AID mutants	Mutation type	Mutation location	Patient data IgM (g/l)	IgG (g/l)	IgA (g/l)	SHM (%)	*In vitro* assay CSR (%)	γ_1 CT	SHM (%)
1	Wild-type hAID							100	++++	100
	Wild-type mAID							130.0 ± 4.2	++++	132.0 ± 17.7
	Empty vector							1.1 ± 0.7	–	0
2	Normal			0.5–1.1	5–12	0.3–1.3	2.5–6.3			
	P1	T	M	4.5	<0.06	<0.07	0	2.0 ± 0.9	–	0.5 ± 0.5
	P7, P11, P12, P18	R	A	1.6–17	<0.5	<0.07	0.9(P18)	1.3 ± 0.8	–	0.5 ± 0.5
	P6, P8	T	L	8–9	0.06–0.3	<0.07	0.76(P8)	1.7 ± 0.7	–	0
	P9, P10	R	A	10–11	0.1–0.5	<0.02		1.4 ± 0.9	–	0
	P13	R	L	34	0.05	<0.02		4.6 ± 0.3	–	0.5 ± 0.5
	P16	R	M	10	1.3	0.2		3.8 ± 3.2	–	0.5 ± 0.5
	P17	T	H	37	<0.02	<0.02	0	2.7 ± 1.8	–	0.5 ± 0.5
	P19	R	M	30	<0.4	<0.1	0	2.1 ± 1.7	–	0.5 ± 0.5
	P20	I	P	5.5	0.1	0	3.4	3.2 ± 1.1	–	71.0 ± 23.4
3	Normal			0.3–1.9	8.7–17	1.1–4.1	0.96–2.6			
	JP8A/JB8B	R/F	L/P	19	<0.02	<0.01	1.3			
	JP8A							4.2 ± 3.5	–	0.8 ± 0.75
	JP8B							4.5 ± 2.5	–	70.0 ± 8
	JP3–JP7	R	L	11–64	<0.1	<0.06	0–0.34	1.8 ± 0.9	–	0.5 ± 0.5
	JP41[a]	T	P	1.6	1.6	0.29		6.6 ± 2	+	75.0 ± 15
	JP42[a]	T	P	2.9	2.8	2.2				
	JP43[a]	T	P	11.3	0.28	<0.05				
4	195	R	M					2.1 ± 1.1	–	0
	202	R	H/P					24.1 ± 3	++	6.9 ± 2.5
	203	R	H					56.7 ± 17	+++	60.0 ± 5.2

Clinical data except for P19, P20 and JP41–JP43 have been published: group 2, ref. 6; group 3, ref. 34. Human AID (hAID) mutants in group 4 were generated by PCR and selected. SHM in groups 2 and 3 was determined for V_H3-23 and V_H5 transcripts, respectively, as described[6,34]. *In vitro* assays were done four times and the results are presented as mean ± s.d. The γ_1CTs are presented as relative intensities of PCR bands, as shown in **Figure 2b**. T, truncation; R, replacement; I, insertion; F, frameshift; M, cytidine deaminase motif; L, linker; A, active site; H, α-helix; P, pseudoactive site; mAID, mouse AID. [a]heterozygotes of 190X and wild-type.

IgG$^+$ cells by fluorescence-activated cell sorting (FACS) analysis (Fig. 2a). We further confirmed the FACS data by measuring γ1 circle transcripts (γ_1CTs), which are derived from transcription initiated at the $S_{\gamma 1}$ intron promoter ($I_{\gamma 1}$) fused to the C_μ exons in circular DNA looped out as the reciprocal product by CSR to IgG1 (Fig. 2b, ref.37;). All HIGM2 mutants were negative for the CSR activity, except for JP41, which had a very low but detectable CSR activity (Table 1). Mutants 202 and 203 had intermediate CSR activity.

We then measured SHM activity of AID mutants by the *in vitro* SHM assay system using NIH3T3 fibroblasts containing a mutated GFP construct (GFP^m) with a premature termination codon in the middle of the coding region[8]. When wild-type AID was expressed in NIH3T3 fibroblasts containing GFP^m by retroviral vector, reversion mutations in GFP^m were induced and were quantified by FACS for GFP expression. Most mutants that did not have CSR activity also lost SHM activity (Fig. 2c). We found intermediate SHM activity in two mutants, 202 and 203, that had intermediate CSR activity. However, mutants P20, JP41 and JP8B, which almost completely lost their CSR activity, retained strong SHM activity (71–75%) compared with that of wild-type AID (Table 1). By DNA sequencing, we confirmed that P20 and wild-type AID induced similarly frequent mutations (6×10^{-3} per base pair) during 4 weeks of culture. Target bases of these mutations were strongly biased to G/C base pairs (data not shown), as previously reported for mutations induced by ectopic expression of AID[8,38].

We then determined nucleotide sequences of rearranged V_H3-23 genes in CD19$^+$CD27$^+$ B cells of the P20 patient and found mutations with a frequency similar to that of normal individuals (Table 1). The JP8 patient, who had the HIGM2 phenotype but retained almost normal SHM[34], is a heterozygote of the JP8A and JP8B alleles. We analyzed the JP8A allele *in vitro* and found it was completely defective for both CSR and SHM. Thus, the SHM activity in the JP8 patient is attributable to the JP8B allele. JP41, JP8B and P20 mutations result in alterations (deletion, replacement or insertion) of the 8–17 residues located C-terminal to the APOBEC-like C-terminal domain (Fig. 1a,b). These results indicate that the C-terminal 8–17 amino acid residues of AID are essential to CSR but not to SHM activity.

P20 mutant retains deamination activity

As P20, JP41 and JP8B retained SHM activity, they are likely to have cytidine deaminase activity despite the defect in their CSR activity. Indeed, P20 increased mutations in *E. coli* (Fig. 2d). Therefore, it is reasonable to assume that these mutations (P20, JP41 and JP8B) abolished neither DNA binding nor its deamination activity, but instead affected one of functional domains required for interaction of AID with CSR-specific substrates (DNA or RNA) or cofactor proteins. As AID does not show specific binding to RNA *in vitro*[15,17], AID probably requires a CSR-specific cofactor(s) whose interaction with AID is disturbed by the P20, JP41 and JP8B mutations at the C-terminal region. Although there is no direct evidence to indicate that AID requires a SHM-specific cofactor(s), JP3 retained cytidine deaminase activity in *E. coli* (Fig. 2d) but had neither CSR nor SHM activity *in vivo* or *in vitro* (Table 1). It is therefore likely that the SHM activity of AID also requires a cofactor(s) that is probably not necessary for mutagenesis in *E. coli*.

Complex formation of AID

The JP41, JP42 and JP43 patients were heterozygotes of the JP41 and wild-type alleles but they had intermediate HIGM2 phenotypes (Table 1). The JP43 patient had an increase in IgM and reduction in

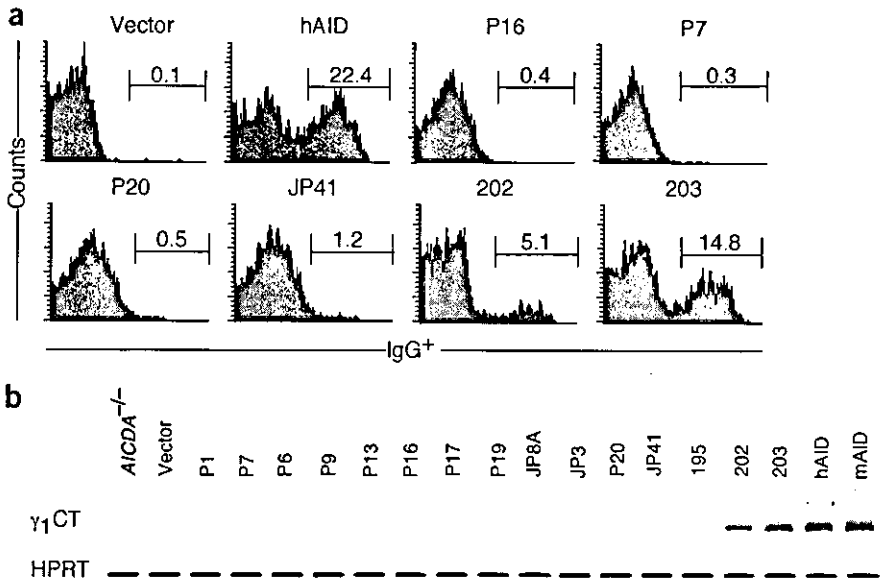

Figure 2 *In vitro* AID mutant CSR and SHM activity. (**a**) *In vitro* assay for CSR. Switching activities of mutants (above FACS profiles). Numbers indicate percentages of IgG$^+$ cells among infectants (GFP$^+$). Data are representative of four experiments. (**b**) γ_1CTs generated by AID mutants. Analysis of γ_1CTs in AID-deficient (*AICDA*$^{-/-}$) spleen B cells infected by retroviruses containing AID mutants (above each lane). Bottom, hypoxanthine guanine phosphoribosyl transferase (HPRT; control of input RNA). Data are representative of four experiments. (**c**) *In vitro* assay for SHM by expression of AID mutants (above FACS profiles). Numbers indicate percentages of NIH3T3 revertants expressing GFP. Data are representative of four experiments. (**d**) Frequencies of Rif^R mutants of *E. coli* generated after culture of *E. coli* clones carrying AID expression constructs or vector control. Expression of recombinant proteins was determined by immunoblot (data not shown). Each point represents the mutation frequency of an independent culture. hAID, human AID.

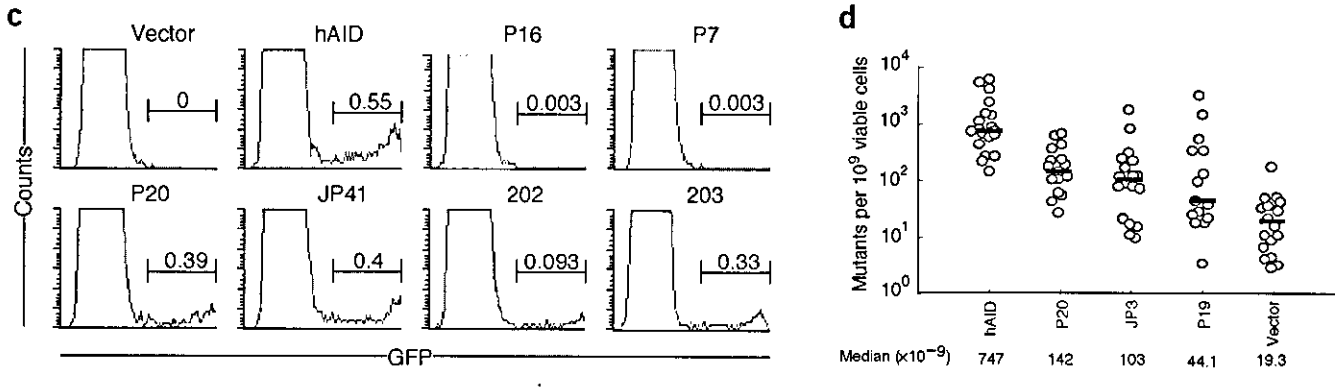

IgG and IgA in the serum, indicating that the JP41 mutant may have a dominant negative effect on CSR. If so, AID might form a dimeric (or multimeric) complex and the inactive complex containing the mutant AID might trap wild-type AID or its cofactors specific to CSR. To examine this possibility, we expressed the AID-GFP fusion protein and mouse AID tagged with the FLAG peptide together in 293T cells and immunoprecipitated their extracts with antibody to FLAG (anti-FLAG) or anti-GFP (Fig. 3a). In both cases, AID molecules with the tag that was not recognized by antibodies used were coprecipitated, indicating that AID forms a dimer or multimer. We found a similar multimeric complex formation between AID and its mutants (P20, JP41, P19 and P7). The complex formation is not due to a particular combination of tags, as we obtained similar results in experiments using AID and AIDER[12], the fusion protein of AID with

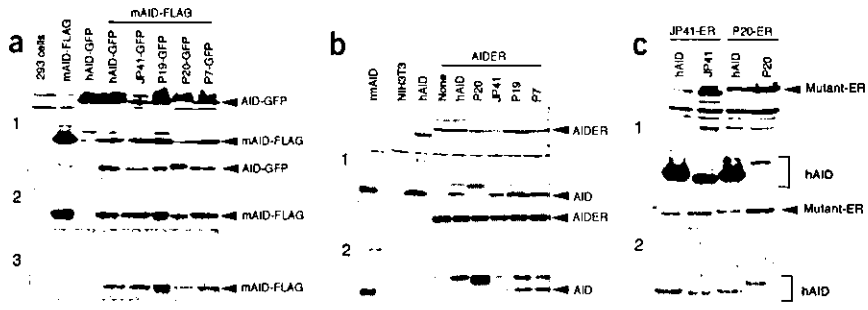

Figure 3 Complex formation of AID. (**a**) Interaction between mouse AID-FLAG and human AID mutants tagged with GFP. 293T cells were transfected with mouse AID-FLAG (+mAID-FLAG) plus human AID (hAID) mutants with GFP. Extracts were analyzed by immunoblot before (1) or after immunoprecipitation with anti-FLAG (2) or anti-GFP (3). Blots were probed with a mixture of AID Abs #1 and #3 (1,2) and with biotinylated anti-FLAG (3). (**b**) NIH3T3 cells expressing mouse AIDER were infected with retrovirus expressing human AID (hAID) mutant. Extracts from tamoxifen-treated cells were immunoprecipitated with anti-FLAG. Blots before (1) and after (2) immunoprecipitation were probed with a mixture of AID Abs #1 and #3. rmAID, recombinant mouse AID. (**c**) Homomultimer of JP41 and P20. JP41 or P20 mutants without tag were transfected with their AIDER construct into 293T cells. After being incubated with 1 μM tamoxifen for 3 h, cells were collected and extracts were used for immunoprecipitation with anti-FLAG. Blots were probed before (1) and after immunoprecipitation (2) with AID Ab #1. All data are representative of three experiments. hAID, human AID. JP41-ER and P20-ER, AIDER forms of JP41 and P20, respectively.

the FLAG-tagged hormone-binding domain of the estrogen receptor (Fig. 3b). Furthermore, the P20 and JP41 mutants were able to form a homomultimeric complex (Fig. 3c).

DISCUSSION

Our results indicate that the activity of AID depends on its interaction with specific cofactors. As AID alone can catalyze deamination of deoxycytidine or cytidine *in vitro* or in *E. coli*, it is less likely that the cofactor(s) of AID is involved in the catalytic function. The AID cofactor(s) is more likely to be involved in recognition of specific substrates in a broad sense, including recruitment of other factors directly associating with substrates. Separate cofactors for CSR and SHM provide AID with a molecular machinery to regulate the two genetic events differentially. Stepwise evolution of CSR and SHM is also consistent with this idea[39]. Then how can AID separately regulate CSR and SHM? RNA-editing enzymes like APOBEC-1 require cofactors for recognition of the target mRNA precursor[40,41]. Similarly, specific cofactors of AID may be required to recognize separate mRNA precursors for CSR and SHM. Two mRNA molecules generated by RNA editing may be translated into endonucleases that have different specificities and cleaving activities for S and V regions. These possibilities exist because CSR and SHM are likely to require double-strand and single-strand (or no) cleavages, respectively. Alternatively, AID could directly deaminate deoxycytidine in DNA[13–17] by recognizing deoxycytidines in immunoglobulin V- and S-region DNA molecules in association with different cofactors. As no specific sequences are required for recognition of target DNA of CSR[20–24] and SHM, it will be important to know how AID and specific cofactors can distinguish deoxycytidine in immunoglobulin V and S regions. It is also possible that AID uses different mechanisms for CSR and SHM. AID requires CSR-specific cofactors for RNA editing to produce CSR-specific endonuclease and SHM-specific cofactors for recognition of the higher-order structure of V-region DNA. In any case, given our results, it is likely that target recognition of AID for CSR and SHM depends on specific cofactors regardless of chemical properties of the target (DNA or RNA).

DNA deamination activity of AID has been reported in *E. coli* and *in vitro*[13–17]. Our studies of AID mutants have indicated that deamination activity in *E. coli* is not sufficient for CSR or SHM in mammalian cells. Similarly, APOBEC-1 was shown to be inactive for CSR and SHM in B cells (T. Eto and T.H., unpublished data), although DNA deamination activity was also found for APOBEC-1 (ref. 42). As target recognition of CSR and SHM, regardless of DNA or RNA, is likely to depend on cofactors but not AID, the base specificity and reaction mechanism studied in *E. coli*[13,14] and *in vitro*[15–17,43] may not apply to the events in B cells.

The requirement for cofactors and dimer formation of AID are reminiscent of RNA-editing enzymes like APOBEC-1 and adenosine deaminase acting on RNA[44]. APOBEC-1 is known to form a dimer[35] and to require APOBEC-1 complementation factor for recognition of RNA target[40,41]. Adenosine deaminase acting on RNA also forms a dimer and contains a large RNA-recognition domain[45,46]. Another unique feature of APOBEC-1 is the formation of a large protein complex (27S) called editosome for RNA editing[47]. Although it is not known whether AID also forms such a large complex as APOBEC-1, AID is likely to interact with several cofactor proteins in addition to CSR-specific cofactor(s), as loss-of–function mutations are found in the α-helix and linker regions and at least some of them did not abolish deamination activity (H.N. and T.H., unpublished data). Although isolation of protein factors associating with AID has been attempted, no positive results have been reported. However, our results indicate the presence of CSR-specific cofactors. The fact that AID forms a multimeric complex is essential for understanding how the putative cofactors interact with AID. The cofactor may interact with the three-dimensional surface of multimeric AID but not with that of monomeric AID. A definitive conclusion about the target of AID awaits the isolation of AID cofactors, as it is the cofactor but not AID itself that recognizes the target.

METHODS

***In vitro* assays for CSR and SHM.** Retrovirally mediated expression of AID mutants using pMX-AID-IRES-GFP constructs has been described[36]. For CSR, stimulated and infected AID-deficient spleen B cells positive for both B220 and GFP were analyzed for surface IgG expression by FACS 3 d after infection. Cells were stained with biotinylated anti-IgG1 and anti-IgG3, followed by incubation with phycoerythrin-labeled streptavidin and allophycocyanin-labeled anti-CD45R (B220). In separate experiments, γ_1CTs in AID-deficient spleen B cells infected with AID mutant retroviruses were assessed[37]. Total RNA was extracted from infected AID-deficient spleen B cells and cDNA was synthesized by RT-PCR. Amplification of γ_1CT was done using a pair of primers: CμR (5′-ATTGGTGCTBGGGCAGGAAGT-3′) and γ_1CT (5′-GGCCCTTCCAGATC TTTGAG-3′). SHM assays were done as described[8]. NIH3T3 cells carrying GFP^m were infected with AID mutants in the pFB (STRATAGENE) retroviral expression vector[8]. After 7 d, cells were analyzed for expression of GFP by FACS.

Deamination activity of AID in *E. coli*. Wild-type and mutated AID cDNA were cloned into the *Nco*I and *Eco*RI sites of the pET-16b (Novagen) expression vector and were used for transformation of *E. coli*. AID expression in *E. coli* increases mutation frequencies by direct deamination of DNA[13]. Rifampicin-resistance (Rif^R) mutants were generated by mutation accumulation in the RNA polymerase gene. *E. coli* strain BL21 (DE3) carrying the AID expression construct or the vector control was cultured for 8 h in Luria-Bertani medium supplemented with 100 μg/ml ampicillin, and Rif^R clones were selected on Luria-Bertani agar containing 100 μg/ml rifampicin and 100 μg/ml ampicillin[13,42]. Mutation frequencies were measured by determining the median number of colony-forming cells surviving selection per 1×10^9 viable cells plated.

Assays for AID complex formation. 293T cells were transfected at a ratio of 1:1 with AID and its mutants differentially tagged with FLAG or GFP or without a tag. Cells were collected 3 d after transfection and extracts were coimmunoprecipitated using either anti-FLAG or anti-GFP. In another experiment, a stable NIH3T3 cell line expressing mouse AIDER[12], which contains a FLAG tag, was infected with AID mutants in pMX-AID-IRES-GFP. Cells with high expression of GFP were sorted, induced by 1 μM tamoxifen for 3 h and used for immunoprecipitation with anti-FLAG. Precipitates were analyzed by immunoblot.

HIGM2 patient samples. Informed consent to use the clinical and DNA analysis results for scientific studies was obtained from all patients. Studies of HIGM2 patient samples were approved by the Comit Consultatif de Protection des Personnes participant une Recherche Biomedicale (Ile de France Paris-Saint-Antoine) and the Ethical Committee of Tokyo Medical and Dental University.

ACKNOWLEDGMENTS

We thank M. Nakata, T. Toyoshima and E. Inoue for technical support; T. Nishikawa and Y. Shiraki for help in preparing the manuscript; S. Fagarasan, B. Meek and R. Shinkura for critical reading of the manuscript; and P. Lane for clinical support of patients. This investigation was supported by The Japan Society for the Promotion of Science (to V.-T.T.) and Center-of-Excellence grants from Minister of Education, Culture, Sports, Science and Technology.

COMPETING INTERESTS STATEMENT

The authors declare that they have no competing financial interests.

Received 18 June; accepted 15 July 2003
Published online at http://www.nature.com/natureimmunology/

1. Honjo, T., Kinoshita, K. & Muramatsu, M. Molecular mechanism of class switch recombination: linkage with somatic hypermutation. *Annu. Rev. Immunol.* **20**, 165–196 (2002).

2. Kinoshita, K. & Honjo, T. Linking class-switch recombination with somatic hypermutation. *Nat. Rev. Mol. Cell Biol.* **2**, 493–503 (2001).
3. Reynaud, C.A., Aoufouchi, S., Faili, A. & Weill, J.C. What role for AID: mutator, or assembler of the immunoglobulin mutasome? *Nat. Immunol.* **4**, 631–638 (2003).
4. Muramatsu, M. *et al.* Specific expression of activation-induced cytidine deaminase (AID), a novel member of the RNA-editing deaminase family in germinal center B cells. *J. Biol. Chem.* **274**, 18470–18476 (1999).
5. Muramatsu, M. *et al.* Class switch recombination and hypermutation require activation-induced cytidine deaminase (AID), a potential RNA editing enzyme. *Cell* **102**, 553–563 (2000).
6. Revy, P. *et al.* Activation-induced cytidine deaminase (AID) deficiency causes the autosomal recessive form of the Hyper-IgM syndrome (HIGM2). *Cell* **201**, 565–575 (2000).
7. Okazaki, I.M., Kinoshita, K., Muramatsu, M., Yoshikawa, K. & Honjo, T. The AID enzyme induces class switch recombination in fibroblasts. *Nature* **416**, 340–345 (2002).
8. Yoshikawa, K. *et al.* AID is a hypermutator of actively-transcribed genes in fibroblasts. *Science* **296**, 2033–2036 (2002).
9. Arakawa, H., Hauschild, J. & Buerstedde, J.M. Requirement of the activation-induced deaminase (AID) gene for immunoglobulin gene conversion. *Science* **295**, 1301–1306 (2002).
10. Harris, R.S., Sale, J.E., Petersen-Mahrt, S.K. & Neuberger, M.S. AID is essential for immunoglobulin V gene conversion in a cultured B cell line. *Curr. Biol.* **12**, 435–438 (2002).
11. Muto, T., Muramatsu, M., Taniwaki, M., Kinoshita, K. & Honjo, T. Isolation, tissue distribution, and chromosomal localization of the human activation-induced cytidine deaminase (AID) gene. *Genomics* **68**, 85–88 (2000).
12. Doi, T., Kinoshita, K., Ikegawa, M., Muramatsu, M. & Honjo, T. *De novo* protein synthesis is required for the activation-induced cytidine deaminase function in class-switch recombination. *Proc. Natl. Acad. Sci. USA* **100**, 2634–2638 (2003).
13. Petersen-Mahrt, S.K., Harris, R.S. & Neuberger, M.S. AID mutates *E. coli* suggesting a DNA deamination mechanism for antibody diversification. *Nature* **418**, 99–103 (2002).
14. Ramiro, A.R., Stavropoulos, P., Jankovic, M. & Nussenzweig, M.C. Transcription enhances AID-mediated cytidine deamination by exposing single-stranded DNA on the nontemplate strand. *Nat. Immunol.* **4**, 452–456 (2003).
15. Dickerson, S.K., Market, E., Besmer, E. & Papavasiliou, F.N. AID mediates hypermutation by deaminating single stranded DNA. *J. Exp. Med.* **197**, 1291–1296 (2003).
16. Chaudhuri, J. *et al.* Transcription-targeted DNA deamination by the AID antibody diversification enzyme. *Nature* **422**, 726–730 (2003).
17. Bransteitter, R., Pham, P., Scharff, M.D. & Goodman, M.F. Activation-induced cytidine deaminase deaminates deoxycytidine on single-stranded DNA but requires the action of RNase. *Proc. Natl. Acad. Sci. USA* **100**, 4102–4107 (2003).
18. Di Noia, J. & Neuberger, M.S. Altering the pathway of immunoglobulin hypermutation by inhibiting uracil-DNA glycosylate. *Nature* **419**, 43–48 (2002).
19. Rada, C. *et al.* Immunoglobulin isotype switching in inhibited and somatic hypermutation perturbed in UNG-deficient mice. *Curr. Biol.* **12**, 1748–1755 (2002).
20. Azuma, T., Motoyama, N., Fields, L.E. & Loh, D.Y. Mutations of the chloramphenicol acetyl transferase transgene driven by the immunoglobulin promoter and intron enhancer. *Int. Immunol.* **5**, 121–130 (1993).
21. Yelamos, J. *et al.* Targeting of non-Ig sequences in place of the V segment by somatic hypermutation. *Nature* **376**, 225–229 (1995).
22. Kinoshita, K., Tashiro, J., Tomita, S., Lee, C.G. & Honjo, T. Target specificity of immunoglobulin class switch recombination is not determined by nucleotide sequences of S regions. *Immunity* **9**, 849–858 (1998).
23. Tashiro, J., Kinoshita, K. & Honjo, T. Palindromic but not G-rich sequences are targets of class switch recombination. *Int. Immunol.* **13**, 495–505 (2001).
24. Shinkura, R. *et al.* The influence of transcriptional orientation on endogenous switch region function. *Nat. Immunol.* **4**, 435–441 (2003).
25. Reaban, M.E., Lebowitz, J. & Griffin, J.A. Transcription induces the formation of a stable RNA.DNA hybrid in the immunoglobulin α switch region. *J. Biol. Chem.* **269**, 21850–21857 (1994).
26. Mussmann, R., Courtet, M., Schwager, J. & Du Pasquier, L. Microsites for immunoglobulin switch recombination beakpoints from *Xenopus* to mammals. *Eur. J. Immunol.* **27**, 1610–1619 (1997).
27. Tian, M. & Alt, F.W. Transcription-induced cleavage of immunoglobulin switch regions by nucleotide excision repair nucleases *in vitro*. *J. Biol. Chem.* **275**, 24163–24172 (2000).
28. Mizuta, R. *et al.* Molecular visualization of immunoglobulin switch region RNA/DNA complex by atomic force microscope. *J. Biol. Chem.* **278**, 4431–4434 (2003).
29. Yu, K., Chedin, F., Hsieh, C-L., Wilson, T.E. & Lieber, M.R. R-loops at immunoglobulin class switch regions in the chromosomes of stimulated B cells. *Nat. Immunol.* **4**, 442–451 (2003).
30. Faili, A. *et al.* AID-dependent somatic hypermutation occurs as a DNA single-strand event in the BL2 cell line. *Nat. Immunol.* **3**, 815–821 (2002).
31. Peterson, S. *et al.* AID is required to initiate Nbs1/γ-H2AX focus formation and mutations at sites of class switching. *Nature* **414**, 660–665 (2001).
32. Chen, X., Kinoshita, K. & Honjo, T. Variable deletion and duplication at recombination junction ends: implication for staggered double-strand cleavage in class-switch recombination. *Proc. Natl. Acad. Sci. USA* **98**, 13860–13865 (2001).
33. Minegishi, Y. *et al.* Mutations in activation-induced cytidine deaminase in patients with hyper IgM syndrome. *Clin. Immunol.* **97**, 203–201 (2000).
34. Zhu, Y. *et al.* Type two hyper-IgM syndrome caused by mutation in activation-induced cytidine deaminase. *J. Med. Dent. Sci.* **50**, 41–46 (2003).
35. Navaratnam, N. *et al. Escherichia coli* cytidine deaminase provides a molecular model for Apo RNA editing and a mechanism for RNA substrate recognition. *J. Mol. Biol.* **275**, 695–714 (1998).
36. Fagarasan, S., Kinoshita, K., Muramatsu, M., Ikuta, K. & Honjo, T. *In situ* class switching and differentiation to IgA-producing cells in the gut lamina propria. *Nature* **413**, 639–643 (2001).
37. Kinoshita, K., Harigai, M., Fagarasan, S., Muramatsu, M. & Honjo, T. A hallmark of active class switch recombination: Transcript directed by I promoters on looped-out circular DNAs. *Proc. Natl. Acad. Sci. USA* **98**, 12620-12633 (2001).
38. Martin, A. *et al.* Activation-induced cytidine deaminase turns on somatic hypermutation in hybridomas. *Nature* **415**, 802–806 (2002).
39. Flajnick, M.F. Comparative analyses of immunoglobulin genes: surprise and portents. *Nature Rev. Imuunol.* **2**, 688–698 (2002).
40. Mehta, A., Kinter, M.T., Sherman, N.E. & Driscoll, D.M. Molecular cloning of apobec-1 complementation factor, a novel RNA-binding protein involved in the editing of apolipoprotein B mRNA. *Mol. Cell. Biol.* **20**, 1846–1854 (2000).
41. Henderson, J.O., Blanc, V. & Davidson N.O. Isolation, characterization and developmental regulation of the human apobec-1 complementation factor (ACF) gene. *Biochim. Biophys. Acta* **1522**, 22–30 (2001).
42. Harris, R.S., Petersen-Mahrt, S.K. & Neuberger, M.S. RNA editing enzyme APOBEC1 and some of its homologs can act as DNA mutators. *Mol. Cell* **10**, 1247–1253 (2002).
43. Pham, P., Bransteitter, R., Petruska, J. & Goodman, M.F. Processive AID-catalysed cytosine deamination on single-stranded DNA simulates somatic hypermutation. *Nature* **424**, 103–107 (2003).
44. Maas, S., Rich, A. Changing genetic information through RNA editing. *Bioessays* **22**, 790–802 (2000).
45. Gallo, A., Keegan, L.P., Ring, G.M. & O'Connell, M.A. An ADAR that edits transcripts encoding ion channel subunits functions as a dimer. *EMBO J.* **22**, 3421–3430 (2003).
46. Cho, D.S, Yang, W., Lee, J.T., Shiekhattar, R., Murray, J. M. & Nishikura, K. Requirement of dimerization for RNA editing activity of adenosine deaminases acting on RNA. *J. Biol. Chem.* **278**, 17093–17102 (2003).
47. Sowden, M.P. *et al.* The editosome for cytidine to uridine mRNA editing has a native complexity of 27S: identification of intracellular domains containing active and inactive editing factors. *J. Cell Sci.* **115**, 1027–1039 (2002).

nature
immunology

Human uracil–DNA glycosylase deficiency associated with profoundly impaired immunoglobulin class-switch recombination

Kohsuke Imai[1], Geir Slupphaug[2], Wen-I Lee[3,4], Patrick Revy[1], Shigeaki Nonoyama[5], Nadia Catalan[1], Leman Yel[6], Monique Forveille[1], Bodil Kavli[2], Hans E Krokan[2], Hans D Ochs[3], Alain Fischer[1,7] & Anne Durandy[1]

Activation-induced cytidine deaminase (AID) is a 'master molecule' in immunoglobulin (Ig) class-switch recombination (CSR) and somatic hypermutation (SHM) generation, AID deficiencies are associated with hyper-IgM phenotypes in humans and mice. We show here that recessive mutations of the gene encoding uracil–DNA glycosylase (*UNG*) are associated with profound impairment in CSR at a DNA precleavage step and with a partial disturbance of the SHM pattern in three patients with hyper-IgM syndrome. Together with the finding that nuclear *UNG* expression was induced in activated B cells, these data support a model of CSR and SHM in which AID deaminates cytosine into uracil in targeted DNA (immunoglobulin switch or variable regions), followed by uracil removal by UNG.

Antigen-dependent immunoglobulin gene alterations such as CSR and SHM are key events in the adaptation of the B cell response through the modification of effector function and affinity to antigen, respectively. CSR and SHM processes share common steps: chromatin opening of the target regions (immunoglobulin switch (S) and variable (V) regions, respectively) associated with transcription, followed by DNA cleavage, repair and ligation[1,2]. The CSR process is initiated by chromatin opening in S regions located 5′ of the constant (C) region and mediated by cytokine-inducible germline transcription from the intron (I) promoter located 5′ of the S regions. Thereafter, the intervening DNA between the two S regions is excised and the functional transcripts (V_H-C_x) are produced after the recombination process[3].

Further understanding of these pathways at a molecular level has been provided by gene identification in part related to the analysis of a primary immunodeficiency condition, the hyper-IgM syndrome (HIGM). HIGM is characterized by normal or increased serum IgM concentrations associated with low or absent serum IgG, IgA and IgE concentrations, indicating a defect in the CSR process[4]. HIGM is a heterogeneous condition, as several molecular defects result in this syndrome. Deficiencies in CD40L (HIGM1)[5–8] and CD40 (HIGM3)[9] result in impaired T cell–B cell cooperation, leading to defective germinal center formation and impaired CSR. In another HIGM condition (HIGM2), a B cell–specific CSR deficiency has been associated with mutations in *AICDA*, the gene encoding AID[10], which is selectively expressed in B cells from germinal centers[11]. The AID defect leads not only to profoundly impaired CSR but also to defective generation of SHM in the V region of immunoglobulin genes[10]. An identical phenotype has been found in AID-deficient mice[12]. Strong evidence has been provided for involvement of AID in the generation of DNA breaks necessary for both CSR and SHM after germline transcription of the target genes[13,14]. However, its mechanism of action remains controversial. AID was originally proposed to act as an RNA-editing enzyme because of its sequence similarity to APOBEC-1, a cytidine deaminase with well known RNA-editing activity[12]. According to this proposal, endonuclease-encoding RNA would be the potential substrate of AID. However, evidence for DNA-editing activity for AID was provided by an increased frequency of consistent transition mutations in dG-dC pairs in *Escherichia coli* expressing human AID[15]. Moreover, it was demonstrated that *in vitro* AID deaminates cytosine to uracil in single-stranded DNA[16–18]. In addition, indirect evidence for involvement of AID in deamination of cytosine residues has been provided by the description of the immunological abnormalities found in UNG-deficient mice, which are characterized by partially defective CSR and a biased pattern of somatic hypermutation toward transitions at dG-dC nucleotides[19]. The phenotype of UNG-deficient mice could be explained by the defective removal from DNA of the uracil residues generated by the deamination of cytosine residues by AID. We show here that UNG deficiency in humans leads to very profound impairment of CSR and a biased pattern of SHM, demonstrating

[1]Institut National de la Santé et de la Recherche Médicale Unité 429, Hôpital Necker-Enfants Malades, 75015 Paris, France. [2]Department of Cancer Research and Molecular Medicine, Norwegian University of Science and Technology, N-7489 Trondheim, Norway. [3]Department of Pediatrics, University of Washington, Seattle, Washington 98195-6320, USA. [4]Department of Pediatrics, Chang Gung Children's Hospital and University, 333, Taoyuan, Taiwan, China. [5]Department of Pediatrics, National Defense Medical College, 359-8513, Saitama, Japan. [6]Division of Basic and Clinical Immunology, Department of Medicine, University of California, Irvine, California 92697, USA. [7]Unité d'Immunologie-Hématologie et Rhumatologie Pédiatrique, Hôpital Necker-Enfants Malades, 75015 Paris, France. Correspondence should be addressed to A.D. (durandy@necker.fr).

Published online 7 September 2003; doi:10.1038/ni974

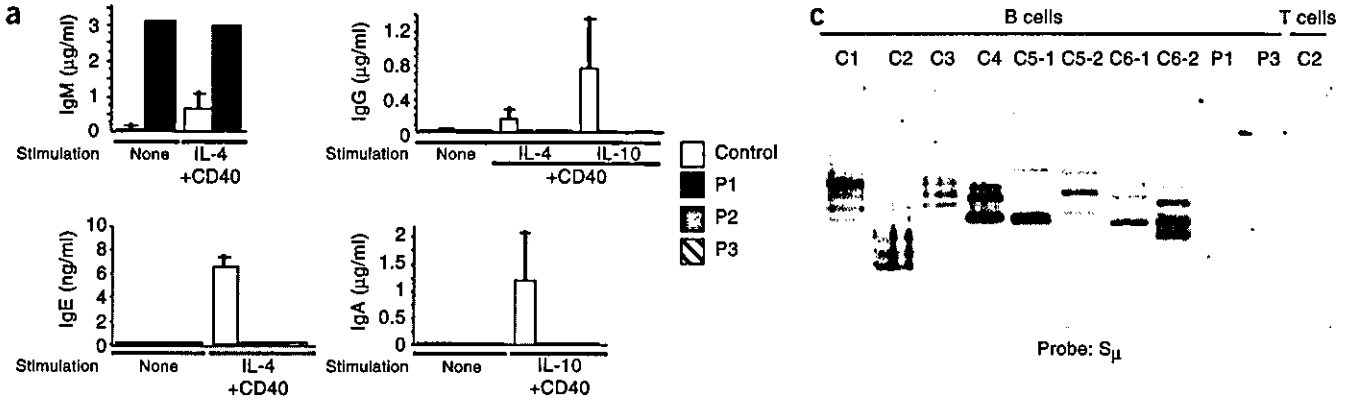

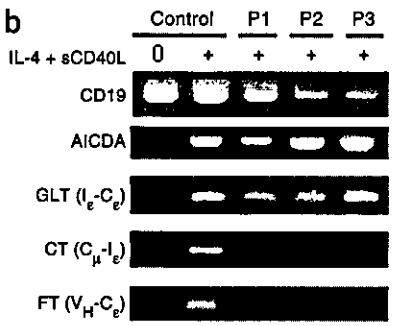

Figure 1 Defective CSR in patients at a precleavage step. (**a**) Impaired *in vitro* CSR in B cells from patients. PBMCs were activated for 12 d in presence of CD40 monoclonal antibody or soluble CD40L plus IL-4 or IL-10. Immunoglobulin production was assessed by enzyme-linked immunosorbent assay. (**b**) Defective expression of IgE circle and functional transcripts in patient B cells. PBMCs were activated for 5 d with soluble CD40L (sCD40L) plus IL-4, and transcripts of genes encoding CD19, AICDA and IgE were detected by RT-PCR. GLT (I_ε-C_ε), germline transcripts; CT (C_μ-I_ε), circle transcripts; FT (V_H-C_ε), functional transcripts. (**c**) Defective CSR-associated DNA double-strand breaks occurrence in Sμ regions in B cells from patients. Viable B cells ($CD19^+$, propidium iodide–negative) from controls (C1–C6), P1 and P3 were purified after 5 d of activation with soluble CD40L plus IL-4. Ligation-mediated PCR products were hybridized with a radiolabeled Sμ probe (exposure time, 18 h). Hybridization revealed several bands in activated B cells from the six controls (two independent results were shown for C5 and C6). T cells activated by anti-CD3 plus IL-2 were used as a negative control. Experiments were done three times for P1 and twice for P3 with same negative results. Ligation-mediated PCR products from controls were cloned and sequenced, and show actual ligation of the linker to Sμ regions at different sites in 56% of clones.

that UNG is essential in this process and supporting the DNA-editing model of AID.

RESULTS

Characterization of molecular defects in *UNG*$^{-/-}$ humans

We studied three unrelated patients (P1, P2 and P3) affected with HIGM, which has characteristics very similar to those of AID deficiency (HIGM2), including susceptibility to bacterial infections, lymphoid hyperplasia, increased serum IgM concentrations and profoundly decreased serum IgG and IgA concentrations (Table 1). B cells from these patients were unable to undergo CSR *in vitro* after activation with antibody to CD40 (anti-CD40) or with soluble CD40 ligand (CD40L) plus interleukin 4 (IL-4) or IL-10 (Fig. 1a). IgG, IgA and IgE molecules as well as IgE functional (V_H-C_ε) and excision circle (C_μ-I_ε) transcripts were almost undetectable in these cells (Fig. 1a,b). These results were in contrast to the ability of these B cells to proliferate and produce large amounts of IgM (data not shown and Fig. 1a). *AICDA* RNA transcripts were present, indicating that the block in CSR was not a consequence of a defect in the signaling leading to *AICDA* expression (Fig. 1b). The possibility of HIGM2 was also excluded, as *AICDA* was unmutated in the three patients (data not shown). IL-4 induction of I_ε-C_ε germline transcription was normal in patient B cells, excluding the possibility of a defect in the CSR initiation step (Fig. 1b). Formation of double-stranded DNA breaks (DSBs) in S regions subsequently occurs in the CSR-associated recombination process[14,20,21]. in the CSR-associated recombination process[14,20,21]. After activation by soluble CD40 ligand plus IL-4, B cells from both patients tested (P1 and P3) repeatedly failed to generate DSBs in Sμ regions, in contrast to control B cells, as shown with a ligation-mediated PCR method[21,22]

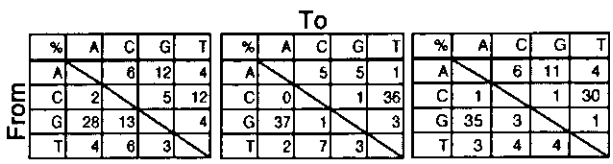

%	Control	P1	P3
Frequency	4.0 (2.6–6.3)	3.4	7.2
Target at dG or dC	63.6 (62–66)	76.8	69.7
Transition at dG or dC	58.9 (57–63)	94.8	93.4
Transversion at dG or dC	41.1 (37–43)	5.2	6.6
Transition at dA or dT	50.4 (33–67)	52.2	49.2
Transversion at dA or dT	49.6 (33–67)	47.8	50.8

Figure 2 SHM frequency and pattern in memory B cells from patients. The frequency and characteristics of SHM in the V_H3-23 region of the IgM were studied in purified $CD19^+CD27^+$ B cells from controls ($n = 7$) and P1 and P3. RT-PCR products amplified by V_H3-23 and C_μ primers amplification were subcloned and sequenced (13 and 10 different clones for P1 and P3, respectively). Bottom, nucleotide changes, shown as percentages. Means and ranges are shown for controls.

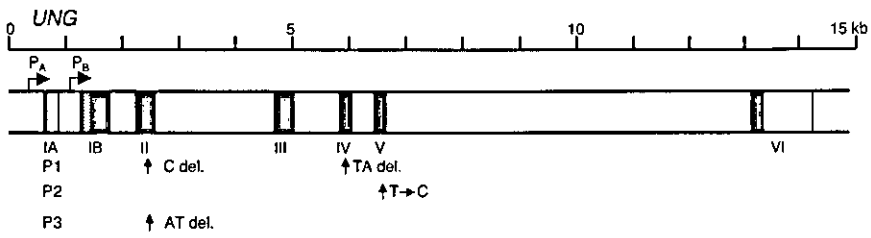

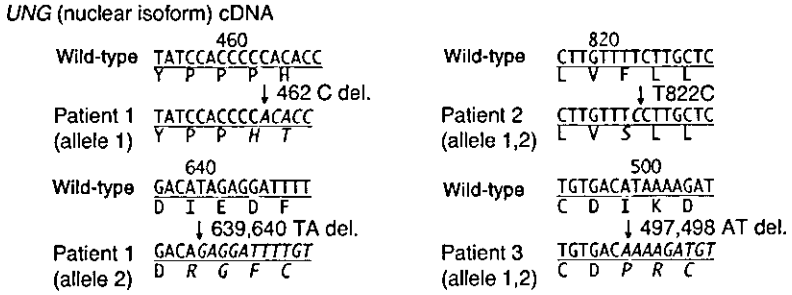

Figure 3 *UNG* mutations in patients. Top, the human *UNG* genomic region. *UNG* has two different promoters (P_B and P_A), leading to two different splice products: the mitochondrial and nuclear isoforms[23]. Below, sequence alterations by mutations and the amino acid changes in the patients (mutation localization on cDNA of nuclear *UNG*). Italics indicate altered nucleotides and amino acids. del., deletion.

(Fig. 1c). Thus, as with AID deficiency[14], this HIGM is characterized by defective cleavage of a targeted S region.

Because AID deficiency is also characterized by defective generation of SHM in the V region of immunoglobulin genes, we analyzed SHM in the V_H3-23 region of IgM in purified B ($CD19^+$) memory ($CD27^+$) cell populations from P1 and P3. The ratio of mutated to unmutated clones was within normal range in memory B cells, as was the frequency of mutations per nucleotide (Fig. 2). However, the SHM pattern was abnormal, as mutations at dG and dC residues were biased toward transitions (dG→dA, dC→dT), whereas at dA and dT residues, the ratio of transitions toward transversions was similar to control values (Fig. 2). Analysis of SHM in P2 B cells was hampered by limited detection of $CD27^+$ peripheral B cells (Table 1).

UNG sequence

The HIGM phenotype in these patients resembles the phenotype described as a consequence of homozygous *Ung* inactivation in mice[19], although in the latter a much milder CSR defect was found. We therefore explored the possibility of UNG deficiency in these three patients. As in mice, human *UNG* has two promoters (P_B and P_A) and two alternative splice products: the mitochondrial isoform, which is ubiquitously expressed, and the nuclear isoform, which is strongly expressed in testis, placenta, thymus and other proliferating cells[23,24]. We sequenced genomic DNA encompassing exons I_A (nuclear *UNG*) and I_B-VI. We found deleterious mutations for all three patients (Fig. 3). We found two heterozygous mutations in P1, both located in the region encoding the UNG catalytic domain, consisting of a C deletion in exon II and a TA deletion in exon IV. Both lead to the generation of premature stop codons (at codons 141 and 224 of nuclear *UNG*, respectively). The mutation in exon II was inherited from an asymptomatic mother, whereas the mutation in exon IV was inherited from asymptomatic father and was also present in healthy sibling. In P2, we found a homozygous missense mutation in exon V (T→C), which leads to a substitution of a phenylalanine (codon 251 of nuclear *UNG*) with a serine in the catalytic domain of UNG. We found the mutation in one allele in each of the healthy parents. To ensure that the mutation in P2 was not a polymorphism, we sequenced *UNG* from 100 chromosomes, including those from controls from the same ethnic group, and found it was normal. In P3, *UNG* analysis showed a homozygous deletion of two nucleotides (AT) in exon II, leading to the generation of a premature stop codon (at codon 159 of nuclear *UNG*). Thus, in all three patients, these recessive mutations were present in the catalytic domain (codons 84–313 of nuclear *UNG*) shared by the mitochondrial and the nuclear isoforms of *UNG*.

Table 1 Serum immunoglobulin concentrations at diagnosis, and $CD19^+$ and $CD27^+$ cells

	P1	P2	P3	Normal range	
Age at diagnosis (years)	7	3	39	3–8	adult
Serum IgM (mg/dl)	740	267	785	50–118	40–230
IgG (mg/dl)	50	<50	209	680–1260	700–1,600
IgA (mg/dl)	48	25	<7	66–162	70–400
$CD19^+$ (/mm^3)[a]	250	860	138	200–2100	100–500
$CD27^+$ (% of $CD19^+$)[a]	17.0	4.6	17.9	10–20	10–40

[a]P1, P2 and P3 were tested at 26, 6 and 40 years of age, respectively.

UNG expression and function

We established Epstein-Barr virus–immortalized lymphoid cell lines (EBV-LCLs) to study UNG expression and function. We were able to detect mitochondrial *UNG* and nuclear *UNG* RNA transcripts by RT-PCR in EBV-LCLs from controls and patients. We also detected nuclear *UNG* in P2 EBV-LCLs, but this was absent or faintly detectable in P1 and P3 EBV-LCLs, indicating that mutations lead to mRNA instability (Fig. 4a). However, immunoprecipitation with an antibody directed to the N-terminal regulatory domain of human UNG (PU1sub) followed by immunoblot analysis with an antibody directed to the C-terminal catalytic domain (PU101) did not detect any material in EBV-LCLs from the three patients (Fig. 4b), demonstrating that all mutations lead to protein instability or compromised translation of the mRNA. Correspondingly, we detected no human UNG activity in EBV-LCLs from the patients (Fig. 4c), in contrast to results obtained with control EBV-LCLs.

Specific induction of nuclear *UNG* expression during CSR

As UNG was required for CSR, we studied the expression of mitochondrial *UNG* and nuclear *UNG* isoforms in B cells before and after activation by soluble CD40L plus IL-4. Resting and activated $CD19^+$ and $CD19^-$ cells had equal expression of mitochondrial *UNG* transcripts (Fig. 4d). In contrast, we only detected nuclear *UNG* transcripts in CSR-induced $CD19^+$ B cells, in correlation with *AICDA* expression (Fig. 4d). We were unable to detect nuclear *Ung* transcripts in mouse spleen naive (IgM^+IgD^+) B ($B220^+$) cells. After 5 d of activation by lipopolysaccharide plus IL-4, they were induced similarly to *Aicda* transcripts. In contrast, mitochondrial *Ung* transcripts were expressed in nonactivated as well as activated B cells (Fig. 4e).

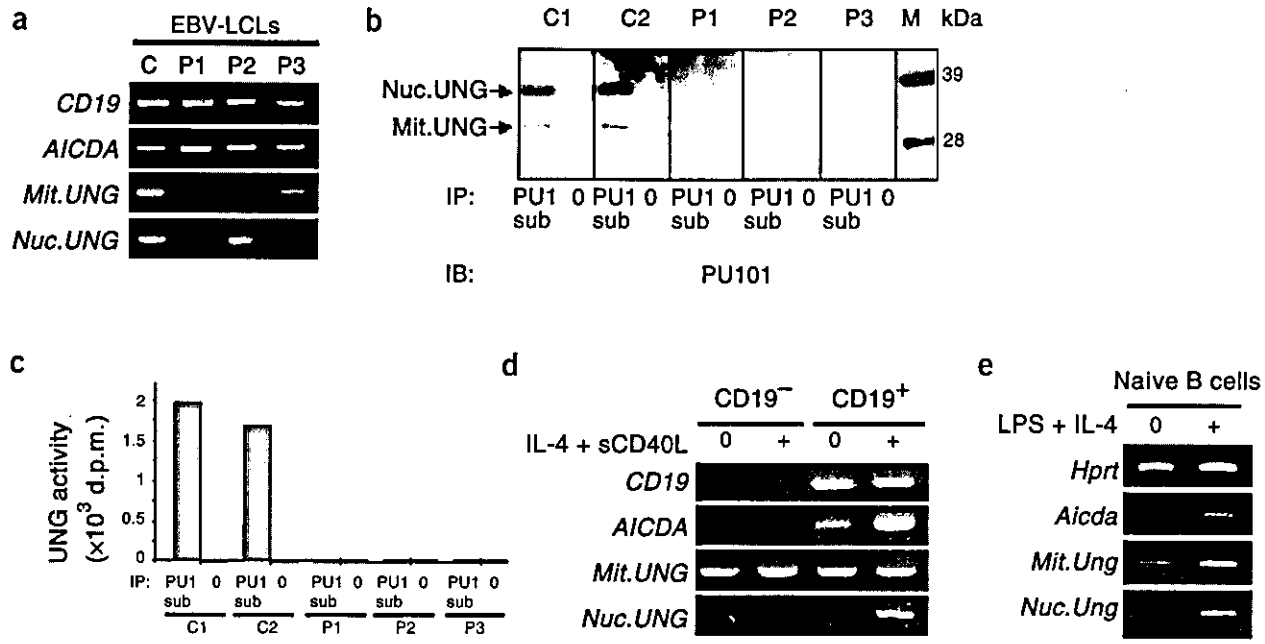

Figure 4 Defective expression and function of UNG in EBV-LCLs of patients. (**a**) *UNG* RNA transcript expression in EBV-LCLs. Mitochondrial and nuclear *UNG* RNA transcript amounts, as detected by RT-PCR, are diminished or absent in P1 (indicating mRNA instability) and normal in P2 and P3. (**b**) UNG protein expression in EBV-LCLs. Immunoblot (IB) of UNG immunoprecipitates from EBV-LCLs fails to demonstrate any mitochondrial or nuclear UNG protein in patients, whereas both forms of UNG are present in the control (C1, C2) cell lines. Identical amounts of total protein were used for immunoprecipitation in all experiments. PU1sub, a non-neutralizing polyclonal antibody directed against the human UNG N-terminal regulatory domain, was used for immunoprecipitation (IP); PU101, a polyclonal antibody against UNG catalytic domain, was used for immunoblot. 0, immunoprecipitation with pre-immune rabbit IgG. M (far right), molecular size markers. (**c**) UNG activity in EBV-LCLs. Specific UNG activity was detected with [^{3}H]dUMP-labeled calf thymus DNA as substrate[47]. UNG activity is present in control EBV-LCLs (C1, C2) after immunoprecipitation with PU1sub. In contrast, there is no activity in EBV-LCLs from patients (P1, P2, P3) or in control beads (0). (**d**) Induction of human nuclear *UNG* in activated control B cells. Transcripts of *CD19*, *AICDA* and *UNG* in control purified CD19$^+$ B cells and CD19$^-$ non-B cells before and after 5 d of *in vitro* activation with soluble CD40L plus IL-4, detected by RT-PCR. Mitochondrial *UNG* is constitutively expressed, whereas nuclear *UNG* is only present in activated CD19$^+$ B cells. (**e**) Induction of mouse nuclear Ung in activated spleen B cells. Mouse spleen naive B cells (B220$^+$IgM$^+$IgD$^+$) were purified and cultured in the presence of lipopolysaccharide (50 μg/ml) plus IL-4 (50 ng/ml) for 5 d. Mitochondrial *Ung* is constitutively expressed, whereas nuclear *Ung* is expressed only in activated B cells. Mit., mitochondrial; Nuc., nuclear.

DISCUSSION

We found UNG deficiency to be linked to a profound inability of human B cells to undergo immunoglobulin CSR associated with qualitative consequences for the pattern of SHM. This recapitulates the UNG-deficient mouse phenotype, although the CSR defect was much more pronounced in humans. Indeed, in mice, the CSR defect is partial *in vivo*, especially found in young mice, whereas it is much more pronounced in *in vitro* experiments[19]. Three possible explanations accounting for this difference can be proposed: other UNGs exert a more redundant activity in mouse B cells; the mismatch-repair enzymes, such as mutS homolog 2 (MSH2) and MSH6, are more important as a surrogate pathway in mice[25,26]; and CSR-deficient mice (such as those deficient in AID, CD40 or CD40L) show a milder phenotype than their human counterparts in terms of serum IgG and IgA isotype concentrations[12,27–29].

As in AID-deficient B cells, the CSR defect in the UNG-deficient B cells seems to occur before S-region cleavage, as evidenced by the lack of DNA breaks. These results strongly support the CSR model in which AID directly deaminates cytosine into uracil residues in the active S regions, followed by uracil removal mediated by UNG, leading to an abasic site. This abasic site can be attacked by an apyrimidinic endonuclease, thus creating a DNA nick[30]. Several groups have concomitantly demonstrated that AID deaminates cytosine in single-stranded DNA but not double-stranded DNA, RNA-DNA hybrids or RNA[16–18]. Transcription of the S region can generate secondary structures such as R-loops, which consist of an RNA-DNA hybrid on the template DNA strand and single-stranded DNA on the nontemplate strand, which may become a target for AID[18,31,32]. It is not known how these DNA breaks on single-stranded DNA result in the DSBs necessary for inter-S-region recombination. AID could exert activity on double-stranded DNA in transcription bubbles[17] or additional, as-yet-unknown factors could be involved[33]. The observation that nuclear *UNG* expression was specifically induced in human and mouse B cells during CSR activation, in parallel with *AICDA* expression, also strengthens, although indirectly, the model described above. In accordance with this model[30], partially defective transversions at dC-dG sites in the SHM process of UNG-deficient B cells would be the consequence of defective error-prone base-excision repair after such site creation at dC residues[30].

Given the sequence similarity to the RNA-editing enzyme APOBEC-1, it has been alternatively proposed that AID edits a putative recombinase-mRNA required for CSR[11]. A protein synthesis–dependent step is downstream from AID activity in CSR, which supports this hypothesis, although this protein synthesis possibly corresponds to the UNG nuclear isoform induction itself[34]. In the RNA-editing hypothesis, UNG might be involved in the base-excision repair process in conjunction with mismatch-repair enzymes, which, when defective, lead to partially impaired CSR and SHM in relevant mouse models[25,26]. Thus, UNG could be part of a complex of proteins, which allows the holding together of cleaved DNA ends[34]; however, this hypothesis does not fit with the defective DSB generation in S regions of UNG-deficient B cells. It is nevertheless possible that

UNG and mismatch-repair enzymes are part of a recombinase complex that mediates additional steps of CSR[34]. There are, however, considerable phenotypic differences in humans between UNG deficiencies and deficiencies in mismatch-repair enzymes, such as mutL homolog 1 (MLH1) and MSH2. Recessive mutations in *MLH1* and *MSH2* predispose to cancer but not to infections[35–38]. Although further studies of CSR status should be done in MLH1- and MSH2-deficient patients, this discrepancy indicates a much more dominant function for UNG in CSR than for mismatch repair enzymes. The profound defect of CSR in UNG-deficient human B cells strongly indicates that other enzymes with UNG activity, including cyclin-like UNG (UNG2)[39,40], single-strand-selective monofunctional UNG 1 (SMUG1)[41], thymine-DNA glycosylase (TDG)[42] and methyl-CpG binding domain protein 4 (MBD4)[43], cannot compensate for UNG deficiency in humans. Moreover, MBD4 deficiency in mice does not impair B cell responses[44]. Although *UNG* mutations in patients have not been directly shown to cause HIGM, the possibility that the nuclear isoform of UNG is involved in CSR is further supported by the observation of its specific induction during *in vitro* B cell activation. In conclusion, the finding that recessive *UNG* mutations are associated with impaired CSR in human B cells and a partially modified pattern of SHM provides further insight into our understanding of the mechanisms underlying secondary immunoglobulin gene alterations in the development of antigen-specific B cell responses.

METHODS

Patients. P1, born to a nonconsanguineous family, presented with recurrent upper and lower respiratory tract infections that had occurred since early childhood. At 7 years of age, the patient was diagnosed with HIGM. A persistent cervical lymph node hyperplasia was noted. The patient is now 27 years old and well on intravenous immunoglobulin (IVIG) treatment. P2, born to a nonconsanguineous family, was diagnosed with HIGM at 3 years of age. The patient is now 6 years old and well controlled on IVIG treatment. P3, born to first-cousin parents, had recurrent upper respiratory tract infections and chronic epididymitis. Cervical and mediastinal lymph node hyperplasia was noted. Antibody titers to pneumococcal and tetanus antigens were found to be decreased, leading to the diagnosis of HIGM when this patient was 39 years of age. The patient is now 40 years old and well on IVIG. All patients have normal T cell counts and functions. Activated T cells had normal expression of CD40L after activation (data not shown). Informed consent was obtained from P1 and P3 and from the parents of P2 for this study, which was approved by the Comité Consultatif de Protection des Personnes participant à une Recherche Biomedicale (Ile de France Paris-Saint-Antoine).

Activation of B cells. Lymphocyte subsets were analyzed as described[45]. Peripheral blood mononuclear cells (PBMCs) were separated by Ficoll-Hypaque density centrifugation (Lymphoprep; Axis-Shield PoC AS). PBMCs were activated *in vitro* with CD32 (FcγRII)-transfected, irradiated L cells (a gift from F. Brière, Schering-Plough) in the presence of anti-CD40 or control IgG (500 ng/ml; Diaclone) or soluble CD40L (500 ng/ml; a gift from Immunex) in combination with IL-4 (100 U/ml; R&D systems) or IL-10 (100 ng/ml, R&D systems). Proliferation was assessed at 5 d by [^{3}H]thymidine uptake. Expression of the genes encoding CD19, AICDA and IgE (GLT, I_ε-C_ε, germline transcripts; CT, C_μ-I_ε, circle transcripts; FT, V_H-C_ε, functional transcripts) was assessed by RT-PCR with the conditions and primers described[10,45] after 5 d of activation with soluble CD40L plus IL-4. *In vitro* production of immunoglobulins (IgM, IgG, IgA and IgE) was assessed by enzyme-linked immunosorbent assay at day 12 in the culture supernatants[45].

Spleen lymphocytes from 6-month-old C57BL/6 mice were isolated by Ficoll-Hypaque gradient centrifugation (NycoPrep 1.077A, Axis-Shield PoC AS). Naive B cells (B220$^+$IgM$^+$IgD$^+$) were separated by FACStarPLUS cell sorter (Becton Dickinson) with the following antibodies: biotinylated anti-mouse B220/CD45R (RA3-6B2; BD Pharmingen), fluorescein isothiocyanate (FITC)-conjugated F(ab')$_2$ fragment goat anti-mouse IgM (Jackson ImmunoResearch Laboratories), phycoerythrin (PE)-conjugated rat anti-mouse IgD (Southern Biotechnology Associates) and PE-Cy5-conjugated streptoavidin (BD Pharmingen). Naive B lymphocytes (1×10^6/ml) were activated for 5 d with lipopolysaccharide (50 μg/ml, *Escherichia coli* serotype 026:B6; Sigma) plus recombinant mouse IL-4 (50 ng/ml; R&D Systems).

Detection of DSBs in the Sμ region of the immunoglobulin locus. PBMCs were activated with soluble CD40L plus IL-4. After 5 d of culture, CD19$^+$ B cells were purified by sorting in the presence of propidium iodide to eliminate dead cells. A ligation-mediated PCR method was used to identify DSBs as described[21,22]. Agarose plugs containing genomic DNA (corresponding to 15×10^3 cells/lane) were ligated to a double-stranded linker. Ligated products were amplified by a semi-nested PCR with Sμ-specific and linker primers. PCR products were hybridized with a radiolabeled Sμ probe and detected with phosphorimager FLA3000 (exposure time, 18 h; Fujifilm). T cells activated for 7 d with anti-CD3 plus IL-2 were used as a negative control. Cloning and sequencing of ligation-mediated PCR products from controls were cloned and sequenced as described[21].

Somatic hypermutation in the variable region of IgM. The frequency and characteristics of SHM in the V_H3-23 region of IgM were studied in purified CD19$^+$CD27$^+$ B cells as described[10]. RT-PCR products of the V_H3-23 region obtained with V_H3-23 and C_μ primers were subcloned and sequenced with the Big Dye DNA sequencing kit (Applied Biosystems) and an automated genetic analyzer (ABI PRISM 377; Applied Biosystems).

Sequence analysis of human *UNG*. Genomic DNA was amplified by PCR with primers directed to intronic or noncoding sequences of *UNG*. PCR products were directly sequenced (primers and conditions for PCR and sequence have been published[46]).

Expression and activity of UNG. *UNG* mRNA transcripts were detected by RT-PCR with primers for mitochondrial *UNG* (36F, 5′-CCGCTCCAGTTTA GAACCTA-3′, and 7Rc, 5′-ACAGCAGCTTCTCAAAGGCC-3′) and nuclear *UNG* (74F, 5′-ATCGGCCAGAAGACGCTCTA-3′, and 7Rc). PCR was completed in 40 cycles (94 °C for 1 min; 62 °C for mitochondrial *UNG* or 65 °C for nuclear *UNG* for 1 min; 72 °C for 2 min). In some experiments, *AICDA* and *UNG* transcripts were tested in sorted CD19$^+$ B cells and CD19$^-$ non-B cells before and after 5 d of activation by soluble CD40L plus IL-4.

Mouse *Ung* mRNA transcripts were detected by RT-PCR with primers for mouse mitochondrial *Ung* (45F, 5′-CGGCGGTCTTTGCGGTTG-3′, and UngR, 5′-GACAACCTTCACATCTCG-3′) and mouse nuclear *Ung* (72F, 5′-ATCGGCCAGAAGACCCTATA-3′, and mUng/exIVR, 5′-CCCACCCTGAC AAATCCCCA-3′). PCR was completed in 40 cycles (94 °C for 1 min; 52 °C for 1 min; 72 °C for 2 min). Transcripts of mouse *Aicda* and *Hprt* (hypoxanthine guanine phosphoribosyl transferase) were detected as described[12].

For analysis of UNG protein, cell-free extracts from EBV-LCLs were immunoprecipitated with magnetic protein A Dynabeads (Dynal) covalently attached to a non-neutralizing polyclonal antibody (PU1sub) directed against the entire human nuclear isoform of UNG and part of the human mitochondrial UNG N-terminal regulatory sequence. Control beads were labeled with the same amount of preimmune IgG from the same rabbit. After polyacrylamide electrophoresis of the eluted immunoprecipitates and electrotransfer to PVDF membranes (Immobilon; Millipore), UNG proteins were detected with a primary polyclonal antibody (PU101) directed against the UNG catalytic domain[47] and secondary horseradish peroxidase–labeled swine anti-rabbit IgG (DakoCytomation) and finally with SuperSignal West femto (Pierce Biotechnology), and were visualized in a Kodak 2000R Image station (Eastman Kodak Company). For specific analysis of UNG activity, cell free extracts from EBV-LCLs of controls and patients were incubated with PU1sub polyclonal antibody or preimmue IgG-labeled beads. After thorough washing, the beads were analyzed for UNG activity by measurement of the released uracil from the assay buffer containing [^{3}H]dUMP-labeled calf thymus DNA substrate[47].

UniGene accession numbers. Human *UNG*, Hs.78853; human mitochondrial *UNG*, NM_003362; human nuclear *UNG*, NM_080911; mouse mitochondrial *Ung*, X99018; mouse nuclear *Ung*, Y08975.

ACKNOWLEDGMENTS

We thank O. Hermine (Paris, France) and M. Endou (Iwate, Japan) for referral of patients. This work was supported by grants from Institut National de la Santé et de la Recherche Médicale, Association pour la Recherche sur le Cancer, la Ligue Contre le Cancer, the European Economic Community (contract QLG1-CT-2001-01536- IMPAD), the Research Council of Norway, the Norwegian Cancer Association, the Svanhild and Arne Must Fund for Medical Research and the Louis Jeantet Foundation, and by grants from the National Institutes of Health (HD 17427-33), the March of Dimes Birth Defects Foundation (96-0330), the Immunodeficiency Foundation and the Jeffrey-Modell Foundation. P.R. is a scientist from Centre National de la Recherche Scientifique (Paris, France). N.C. is supported by the Association pour la Recherche sur le Cancer.

COMPETING INTERESTS STATEMENT

The authors declare that they have no competing financial interests.

Received 19 May; accepted 23 July 2003
Published online at http://www.nature.com/natureimmunology/

1. Manis, J.P., Tian, M. & Alt, F.W. Mechanism and control of class-switch recombination. *Trends Immunol.* **23**, 31–39 (2002).
2. Honjo, T., Kinoshita, K. & Muramatsu, M. Molecular mechanism of class switch recombination: linkage with somatic hypermutation. *Annu. Rev. Immunol.* **20**, 165–196 (2002).
3. Kinoshita, K. & Honjo, T. Linking class-switch recombination with somatic hypermutation. *Nat. Rev. Mol. Cell Biol.* **2**, 493–503 (2001).
4. Durandy, A. Hyper-IgM syndromes: a model for studying the regulation of class switch recombination and somatic hypermutation generation. *Biochem. Soc. Trans.* **30**, 815–818 (2002).
5. Korthauer, U. *et al.* Defective expression of T-cell CD40 ligand causes X-linked immunodeficiency with hyper-IgM. *Nature* **361**, 539–541 (1993).
6. DiSanto, J.P., Bonnefoy, J.Y., Gauchat, J.F., Fischer, A. & de Saint Basile, G. CD40 ligand mutations in X-linked immunodeficiency with hyper-IgM. *Nature* **361**, 541–543 (1993).
7. Aruffo, A. *et al.* The CD40 ligand, gp39, is defective in activated T cells from patients with X-linked hyper-IgM syndrome. *Cell* **72**, 291–300 (1993).
8. Allen, R.C. *et al.* CD40 ligand gene defects responsible for X-linked hyper-IgM syndrome. *Science* **259**, 990–993 (1993).
9. Ferrari, S. *et al.* Mutations of CD40 gene cause an autosomal recessive form of immunodeficiency with hyper IgM. *Proc. Natl. Acad. Sci. USA* **98**, 12614–12619 (2001).
10. Revy, P. *et al.* Activation-induced cytidine deaminase (AID) deficiency causes the autosomal recessive form of the Hyper-IgM syndrome (HIGM2). *Cell* **102**, 565–575 (2000).
11. Muramatsu, M. *et al.* Specific expression of activation-induced cytidine deaminase (AID), a novel member of the RNA-editing deaminase family in germinal center B cells. *J. Biol. Chem.* **274**, 18470–18476 (1999).
12. Muramatsu, M. *et al.* Class switch recombination and hypermutation require activation-induced cytidine deaminase (AID), a potential RNA editing enzyme. *Cell* **102**, 553–563 (2000).
13. Bross, L., Muramatsu, M., Kinoshita, K., Honjo, T. & Jacobs, H. DNA double-strand breaks: prior to but not sufficient in targeting hypermutation. *J. Exp. Med.* **195**, 1187–1192 (2002).
14. Petersen, S. *et al.* AID is required to initiate Nbs1/g-H2AX focus formation and mutations at sites of class switching. *Nature* **414**, 660–665 (2001).
15. Petersen-Mahrt, S.K., Harris, R.S. & Neuberger, M.S. AID mutates *E. coli* suggesting a DNA deamination mechanism for antibody diversification. *Nature* **418**, 99–104 (2002).
16. Chaudhuri, J. *et al.* Transcription-targeted DNA deamination by the AID antibody diversification enzyme. *Nature* **422**, 726–730 (2003).
17. Bransteitter, R., Pham, P., Scharff, M.D. & Goodman, M.F. Activation-induced cytidine deaminase deaminates deoxycytidine on single-stranded DNA but requires the action of RNase. *Proc. Natl. Acad. Sci. USA* **100**, 4102–4107 (2003).
18. Ramiro, A.R., Stavropoulos, P., Jankovic, M. & Nussenzweig, M.C. Transcription enhances AID-mediated cytidine deamination by exposing single-stranded DNA on the nontemplate strand. *Nat. Immunol.* **4**, 452–456 (2003).
19. Rada, C. *et al.* Immunoglobulin isotype switching is inhibited and somatic hypermutation perturbed in UNG-deficient mice. *Curr. Biol.* **12**, 1748–1755 (2002).
20. Wuerffel, R.A., Du, J., Thompson, R.J. & Kenter, A.L. Ig Sg3 DNA-specific double strand breaks are induced in mitogen-activated B cells and are implicated in switch recombination. *J. Immunol.* **159**, 4139–4144 (1997).
21. Imai, K. *et al.* Hyper-IgM syndrome type 4 with a B lymphocyte-intrinsic selective deficiency in Ig class-switch recombination. *J. Clin. Invest.* **112**, 136–142 (2003).
22. Papavasiliou, F.N. & Schatz, D.G. Cell-cycle-regulated DNA double-stranded breaks in somatic hypermutation of immunoglobulin genes. *Nature* **408**, 216–221 (2000).
23. Nilsen, H. *et al.* Nuclear and mitochondriaf uracil-DNA glycosylases are generated by alternative splicing and transcription from different positions in the UNG gene. *Nucleic Acids Res.* **25**, 750–755 (1997).
24. Otterlei, M. *et al.* Nuclear and mitochondrial splice forms of human uracil-DNA glycosylase contain a complex nuclear localisation signal and a strong classical mitochondrial localisation signal, respectively. *Nucleic Acids Res.* **26**, 4611–4617 (1998).
25. Ehrenstein, M.R. & Neuberger, M.S. Deficiency in Msh2 affects the efficiency and local sequence specificity of immunoglobulin class-switch recombination: parallels with somatic hypermutation. *EMBO J.* **18**, 3484–3490 (1999).
26. Schrader, C.E., Edelmann, W., Kucherlapati, R. & Stavnezer, J. Reduced isotype switching in splenic B cells from mice deficient in mismatch repair enzymes. *J. Exp. Med.* **190**, 323–330 (1999).
27. Castigli, E. *et al.* CD40-deficient mice generated by recombination-activating gene-2-deficient blastocyst complementation. *Proc. Natl. Acad. Sci. USA* **91**, 12135–12139 (1994).
28. Xu, J. *et al.* Mice deficient for the CD40 ligand. *Immunity* **1**, 423–431 (1994).
29. Kawabe, T. *et al.* The immune responses in CD40-deficient mice: impaired immunoglobulin class switching and germinal center formation. *Immunity* **1**, 167–178 (1994).
30. Di Noia, J. & Neuberger, M.S. Altering the pathway of immunoglobulin hypermutation by inhibiting uracil-DNA glycosylase. *Nature* **419**, 43–48 (2002).
31. Yu, K., Chedin, F., Hsieh, C.L., Wilson, T.E. & Lieber, M.R. R-loops at immunoglobulin class switch regions in the chromosomes of stimulated B cells. *Nat. Immunol.* **4**, 442–451 (2003).
32. Shinkura, R. *et al.* The influence of transcriptional orientation on endogenous switch region function. *Nat. Immunol.* **4**, 435–441 (2003).
33. Fugmann, S.D. & Schatz, D.G. RNA AIDs DNA. *Nat. Immunol.* **4**, 429–430 (2003).
34. Doi, T., Kinoshita, K., Ikegawa, M., Muramatsu, M. & Honjo, T. *De novo* protein synthesis is required for the activation-induced cytidine deaminase function in class-switch recombination. *Proc. Natl. Acad. Sci. USA* **100**, 2634–2638 (2003).
35. Vilkki, S. *et al.* Extensive somatic microsatellite mutations in normal human tissue. *Cancer Res.* **61**, 4541–4544 (2001).
36. Wang, Q. *et al.* Neurofibromatosis and early onset of cancers in hMLH1-deficient children. *Cancer Res.* **59**, 294–297 (1999).
37. Whiteside, D. *et al.* A homozygous germ-line mutation in the human MSH2 gene predisposes to hematological malignancy and multiple cafe-au-lait spots. *Cancer Res.* **62**, 359–362 (2002).
38. Bougeard, G. *et al.* Early onset brain tumor and lymphoma in MSH2-deficient children. *Am. J. Hum. Genet.* **72**, 213–216 (2003).
39. Muller, S.J. & Caradonna, S. Isolation and characterization of a human cDNA encoding uracil-DNA glycosylase. *Biochim. Biophys. Acta* **1088**, 197–207 (1991).
40. Muller, S.J. & Caradonna, S. Cell cycle regulation of a human cyclin-like gene encoding uracil-DNA glycosylase. *J. Biol. Chem.* **268**, 1310–1319 (1993).
41. Nilsen, H. *et al.* Excision of deaminated cytosine from the vertebrate genome: role of the SMUG1 uracil-DNA glycosylase. *EMBO J.* **20**, 4278–4286 (2001).
42. Neddermann, P. *et al.* Cloning and expression of human G/T mismatch-specific thymine-DNA glycosylase. *J. Biol. Chem.* **271**, 12767–12774 (1996).
43. Hendrich, B., Hardeland, U., Ng, H.H., Jiricny, J. & Bird, A. The thymine glycosylase MBD4 can bind to the product of deamination at methylated CpG sites. *Nature* **401**, 301–304 (1999).
44. Bardwell, P.D. *et al.* Cutting edge: the G-U mismatch glycosylase methyl-CpG binding domain 4 is dispensable for somatic hypermutation and class switch recombination. *J. Immunol.* **170**, 1620–1624 (2003).
45. Durandy, A. *et al.* Abnormal CD40-mediated activation pathway in B lymphocytes from patients with hyper-IgM syndrome and normal CD40 ligand expression. *J. Immunol.* **158**, 2576–2584 (1997).
46. Kvaloy, K. *et al.* Sequence variation in the human uracil-DNA glycosylase (UNG) gene. *Mutat. Res.* **461**, 325–338 (2001).
47. Slupphaug, G. *et al.* Properties of a recombinant human uracil-DNA glycosylase from the UNG gene and evidence that UNG encodes the major uracil-DNA glycosylase. *Biochemistry* **34**, 128–138 (1995).

CD40 ligand is a critical effector of Epstein–Barr virus in host cell survival and transformation

Ken-Ichi Imadome*†, Masaki Shirakata*‡, Norio Shimizu§, Shigeaki Nonoyama¶‖, and Yuji Yamanashi*‡**

Departments of *Cell Regulation and §Virology, Medical Research Institute, ¶Department of Pediatrics and Developmental Biology, and **School of Biomedical Science, Tokyo Medical and Dental University, Tokyo 113-8510, Japan

Edited by George Klein, Karolinska Institute, Stockholm, Sweden, and approved April 24, 2003 (received for review March 8, 2003)

Epstein–Barr virus (EBV), implicated in numerous human diseases, including lymphoid malignancies, persistently infects peripheral B cells and transforms them into lymphoblastoid cell lines. Here we found that EBV equally infected B cells from patients with X-linked hyper IgM syndrome and those from healthy donors; however, it hardly transformed X-linked hyper IgM syndrome B cells, because of the dysfunctional gene of CD40 ligand (CD40L) of the patients. Unlike CD40, CD40L is not usually expressed on B cells. However, we found that EBV infection of normal B cells induced CD40L expression as a critical effector in host cell transformation and survival. Moreover, chronic active EBV infection of peripheral T cells, implicated in T cell malignancies, was associated with ectopic expression of CD40, and, in Jurkat T cells, EBV infection induced CD40 expression. These results suggest that EBV infection induces CD40L/CD40 signaling in host cells, which appears to play an essential role in its persistent infection and malignancies of lymphocytes.

Epstein–Barr virus (EBV), a ubiquitous human lymphotropic herpesvirus, is a cause of lymphoproliferative diseases in immunosuppressed patients and infectious mononucleosis and is tightly associated with lymphoid malignancies such as Burkitt's lymphoma and T cell/natural killer cell lymphoma (1). EBV infection is also associated with epithelial malignancies such as nasopharyngeal carcinoma and gastric carcinoma. An important biological property of EBV, which rationalizes its tight link to cancer, is an ability to transform peripheral B cells in terms of their continuous growth *in vitro* and to establish latently infected lymphoblastoid cell lines (LCLs), which eventually become immortalized (1). LCLs express nine viral proteins: six EBV nuclear antigens (EBNA1–EBNA6) and three latent membrane proteins (LMP1, LMP2A, and LMP2B). Among them, an integral membrane protein, LMP1, is believed to be a key regulator of the B cell transformation, mainly because it transforms fibroblasts or epithelial cells and also induces B cell lymphoma in transgenic mice (1, 2). However, LMP1 expression is insufficient to maintain B cell proliferation, which needs, at least, a second signal (3).

CD40 is a membrane-bound protein of the tumor necrosis factor (TNF) receptor family and is expressed on many cell types including B cells. Its ligand, CD40 ligand (CD40L), is a member of the TNF family and expressed mainly on activated T cells. CD40–CD40L interaction is crucial to B cells for their proliferation, survival, Ig istotype switching, and germinal center reaction upon stimulation by activated T cells (4). For instance, mutations in the CD40L gene were identified as the cause of X-linked hyper IgM syndrome (XHIM), a disease associated with drastic, if not complete, inhibition in T cell-dependent humoral immune responses (4, 5). Mice null for CD40 or CD40L had severe defects not only in their Ig isotype switching, but also in germinal center formation and establishment of B cell memory (4, 6). That we had very few LCLs from XHIM B cells upon EBV infection led us to investigate whether CD40L and CD40 play a role in EBV infection and/or subsequent B cell transformation.

Materials and Methods

Reagents. For flow cytometry, mAbs to CD40 (5C3, PharMingen), CD40L (TRAP1, PharMingen), CD3 (Leu-4, PharMingen), and CD19 (HD37, DAKO) and isotype-matched control Ig (PharMingen) were used. For immunoblot analysis, mAb to LMP1 (S12, a gift from E. Kieff, Harvard Medical School, Boston) (7, 8) and a goat polyclonal antibody to β-actin (I-19, Santa Cruz Biotechnology) were used. For CD40 stimulation in LCL analysis, an agonistic mAb to CD40 (mAb89, Immunotech, Luminy, France) was used (9). For CD40L blocking, CD40Ig, a fusion protein of mouse CD40 (amino acids 1–193) and the Fc region of mouse IgG_{2a}, was used. The CD40Ig was expressed in Sf9 cells by using the baculovirus vector plasmid pFastBac-mCD40/mγ2a (a gift from M. R. Kehry, Boehringer Ingelheim Pharmaceuticals, Ridgefield, CT) and purified to homogeneity (>95%) with protein A-Sepharose (Amersham Pharmacia). The CD40Ig blocked human CD40L, but not IL-4, from stimulating peripheral blood B cell proliferation (data not shown).

Human Peripheral Blood Lymphocytes. Ethical approval was obtained from the ethical boards of the Department of Medicine and Medical Research Institute of Tokyo Medical and Dental University, and informed consent was obtained from all blood donors. B cells were isolated from peripheral blood mononuclear cells (PBMCs) with anti-CD19 Dynabeads M-450 (Dynal, Great Neck, NY) according to the manufacturer's directions. T cells were isolated from PBMCs with mAb to CD3 by using a cell sorter (FACSVantage, Becton Dickinson). Each preparation contained >98% $CD19^+$ or $CD3^+$ lymphocytes.

EBV Infection. EBV was prepared from culture medium of B95–8 cells as described (10) and concentrated (200-fold) in RPMI medium 1640 supplemented with 10% FCS. The virus suspension was filtered (0.45 μm) and recipient cells (2×10^6 to 1×10^7) were incubated in 1 or 5 ml of the suspension for 1 h, then rinsed twice with the culture medium (RPMI medium 1640 supplemented with 10% FCS). The efficiency of infection was >90% as judged by EBNA staining. For inactivation of the EBV genome, 1 ml of virus suspension in a 100-mm dish was irradiated with UV (254 nm) at 1 J/cm² by using a FUNA-UV-LINKER FS-800 (Funakoshi, Tokyo). For mock infection, culture medium was added instead of the EBV suspension.

LCL Assay. After EBV infection, B cells were cultured in 96-well plates (1×10^3 cells per well or as indicated) for 4 weeks. Then,

This paper was submitted directly (Track II) to the PNAS office.

Abbreviations: EBV, Epstein–Barr virus; EBNA, EBV nuclear antigen; CD40L, CD40 ligand; LCL, lymphoblastoid cell line; hpi, hours postinfection; XHIM, X-linked hyper IgM syndrome; CAEBV, chronic active EBV infection; LMP, latent membrane protein.

†Present address: Department of Infectious Diseases, National Research Institute for Child Health and Development, Setagaya-ku, Tokyo 154-8567, Japan.

‡To whom correspondence should be addressed. E-mail: shirakata.creg@mri.tmd.ac.jp or yamanashi.creg@mri.tmd.ac.jp.

Present address: Department of Pediatrics, National Defense Medical College, Tokorozawa-shi, Saitama 359-0042, Japan.

of 96 or 32 wells, the wells containing growing cells (LCL) were enumerated. No LCL was generated in the absence of EBV infection in this assay. In LCL-negative wells, no living cell was observed at 4 weeks postinfection, irrespective of B cell type (normal or XHIM), and another 4 weeks of extended culture did not generate any LCL in those LCL-negative wells. Half of the culture medium was replaced with fresh medium every 3 days.

EBNA Staining. Cytospin slides were prepared from EBV-infected or mock-infected B cells and fixed in acetone/methanol (1:1). Then, EBNAs were visualized by using anticomplement immunofluorescence as described (11). Briefly, the fixed B cells were first treated with human serum to EBNA containing complement (a gift from F. Mizuno, Tokyo Medical University, Tokyo). Then, they were washed and stained with FITC-labeled rabbit polyclonal antibody to human C3c complement (F0201, DAKO).

RT-PCR and Southern Blotting. Total RNA of cells was prepared with ISOGEN (Nippon Gene, Toyama, Japan). RT-PCR was performed with 5 μg total RNA by using the SuperScript OneStep RT-PCR system (Invitrogen). Conditions for the RT reaction and PCR were optimized to produce a specific cDNA product for each gene tested. Primers used were: 5′-TGC CAG CCA GGA CAG AAA CT-3′ (CD40 sense) and 5′-GGG ACC ACA GAC AAC ATC AG-3′ (CD40 antisense), 5′-TGC GGC ACA TGT CAT AAG-3′ (CD40L sense) and 5′-CGG AAC TGT GGG TAT TT-3′ (CD40L antisense). PCR products were subjected to Southern blotting with the following oligonucleotide probes: 5′-AAG AAG GCT GGC ACT GTA-3′ (CD40 probe) and 5′-CAT CTG TGT TAC AGT GGG-3′ (CD40L probe). RT-PCR primers and a probe for EBNA1 have been described (12). RT-PCR primers for β-actin (Takara, Osaka) were purchased.

Apoptosis Assay. After EBV infection, cells were plated to a 96-well plate (1×10^4 cells per well) and cultured for 0, 24, or 48 h in the presence or absence of the reagent(s) indicated in each assay. These cells were stained with acridine orange (2 μg/ml) and ethidium bromide (2 μg/ml) and examined under a fluorescent microscope for counting apoptotic cells, which were identified by nuclear morphology according to an established protocol (13). An apoptotic index was calculated from the results of counting 200 cells in total. Apoptotic cells were otherwise detected as indicated with an ApopTag ISOL kit (Intergen, Purchase, NY), which probes double-strand DNA breaks with a hairpin oligo-DNA probe and T4-DNA ligase.

EBV DNA Assay. Copy numbers of EBV DNA per cellular DNA (μg) in $CD3^+/CD40^-$ or $CD3^+/CD40^{+/-}$ chronic active EBV infection (CAEBV) T lymphocytes were determined by the real-time PCR method with a LightCycler DNA Master Hybridization Probes system (Roche Diagnostics) by using a set of primers, 5′-CGC ATA ATG GCG GAC CTA-3′ and 5′-CAA ACA AGC CCA CTC CCC-3′, and a pair of fluorogenic probes, LC-5′-AAC CAT AGA CCC GCT TCC TG-3′, and 5′-AAA GAT AGC AGC AGC GCA GC-3′-FITC for fluorescence resonance energy transfer-based detection (14). These oligonucleotides were selected from the BWRF1 gene of EBV (1).

Results and Discussion

CD40L Is Indispensable for EBV-Induced B Cell Transformation. Trying to establish LCLs from peripheral B cells of XHIM patients carrying the dysfunctional CD40L gene, we found that EBV infection hardly transformed those B cells into LCLs (Fig. 1 *A* and *B*). This was not caused by a low efficiency of infection because EBV infected XHIM and normal B cells equally and expressed comparable amounts of LMP1 (Fig. 1 *C* and *D*). Furthermore, additional CD40 stimulation restored the transformation of XHIM B cells upon EBV infection (Fig. 1*E*), indicating a critical role for CD40L and CD40 signaling in EBV-mediated B cell transformation. Indeed, CD40Ig, a specific antagonist to CD40L (15), severely impaired transformation of normal peripheral B cells upon EBV infection (Fig. 1*F*). It is also reported that XHIM patients appeared at high risk of developing cytomegalovirus infection but not infection of other herpesviruses, including EBV (16). In contrast, EBV activities were frequently observed in patients with other primary or secondary immune deficiencies (17), implying a role for CD40L in EBV infection. Because peripheral B cells from healthy donors don't express CD40L, we hypothesized that EBV infection induces ectopic expression of functional CD40L on B cells as a critical effector in cellular transformation.

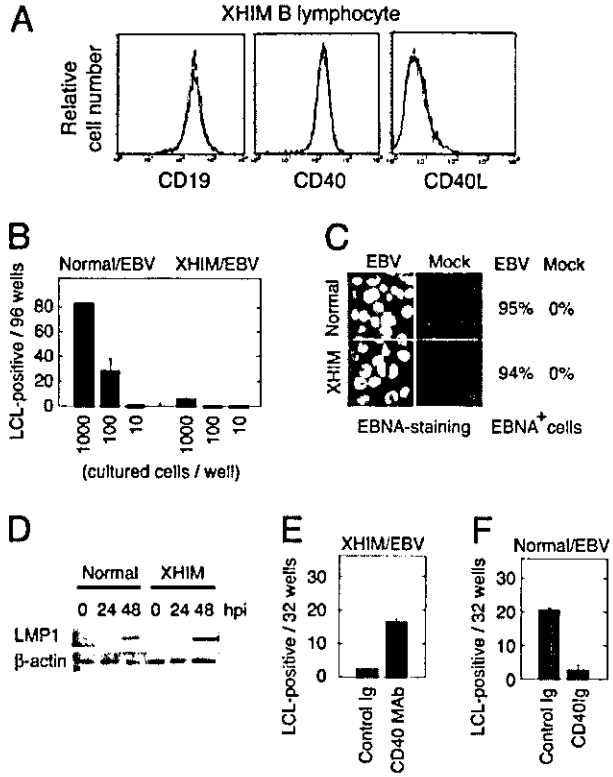

Fig. 1. CD40L is indispensable for EBV-induced B cell transformation. (*A*) EBV-infected (solid line) or mock-infected (dotted lines) XHIM peripheral B cells were subjected to flow cytometry with the indicated mAb at 24 hpi. (*B*) XHIM peripheral B cells generated only marginal numbers of LCLs upon EBV infection in contrast to normal B cells. Data represent mean values and standard errors from sextuplicate experiments of LCL assay. (*C*) EBV equally infected peripheral B cells of XHIM patients and those of healthy donors (Normal). EBNAs were stained with anti-EBNA human serum at 24 hpi, and each staining, in total, showed 95% (122 of 128) or 94% (118 of 126) EBNA-positive ($EBNA^+$) cells in EBV-infected cells. (*D*) LMP1 or β-actin in EBV-infected XHIM or normal peripheral B cells at the indicated hpi was examined by immunoblotting. (*E*) Stimulation of CD40 with an agonistic mAb, mAb89 (10 μg/ml), restored the EBV-induced transformation of XHIM peripheral B cells to LCLs (CD40 mAb). Data represent mean values and standard errors from triplicate experiments of LCL assay. (*F*) Blocking of CD40L with CD40Ig (200 μg/ml) inhibited transformation of normal peripheral B cells to LCLs. Data represent mean values and standard errors from sextuplicate experiments of LCL assay.

EBV Infection Induces Ectopic Expression of CD40L on B Cells. To test our hypothesis, we first studied EBV-negative Ramos B cells upon EBV infection and found that CD40L mRNA was induced as early as 24 h postinfection (hpi) (Fig. 2*A*). Surface expression of CD40L was also confirmed at 48 hpi (Fig. 2*B*). However, EBV

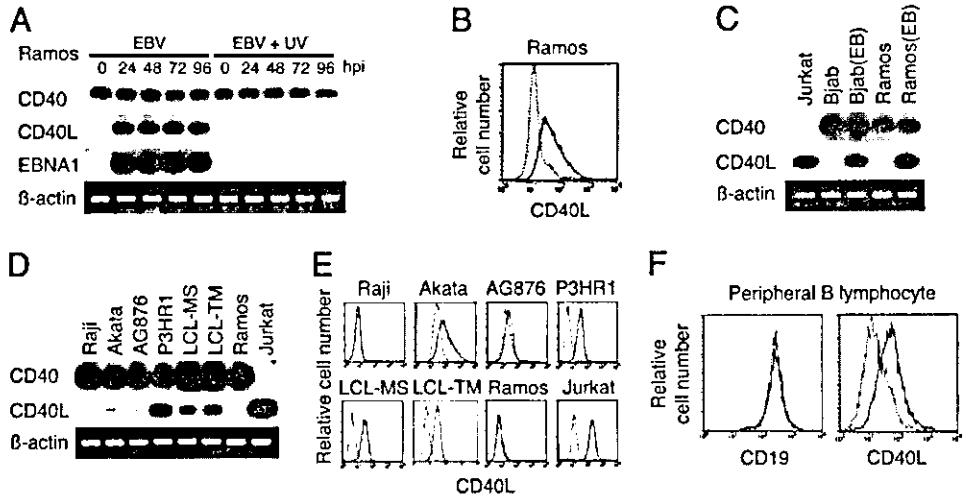

Fig. 2. EBV infection induces ectopic expression of CD40L on B cells. (*A*) Expression of CD40, CD40L, or EBNA1 mRNA in EBV-infected Ramos B cells at the indicated hpi was examined by RT-PCR followed by Southern blotting (EBV). EBV with an UV-inactivated genome induced neither CD40L nor EBNA1 mRNA (EBV+UV). Expression of β-actin mRNA was examined by RT-PCR and visualized by ethidium bromide staining. (*B*) Flow cytometry with mAb to CD40L shows its surface expression on EBV-infected (solid line), but not mock-infected (dotted line), Ramos cells at 48 hpi. (*C*) Expression of the indicated mRNA in the EBV-positive B cells, Bjab(EB) and Ramos(EB), and their EBV-negative parental cells, Bjab and Ramos, was examined as described in *A*. (*D*) Expression of the indicated mRNA in EBV-positive B cells or EBV-negative B or T cells (Ramos or Jurkat) was examined as described in *A*. (*E*) Surface expression of CD40L was examined by flow cytometry with mAb to CD40L (solid line) or isotype-matched control (dotted line). (*F*) Surface expression of CD40L and CD19 on EBV-infected (solid line) or mock-infected peripheral B cells (dotted line) was examined at 24 hpi.

with a UV-inactivated genome induced neither CD40L nor a viral gene, EBNA1, indicating that expression of viral gene(s) is required for CD40L induction (Fig. 2*A*). CD40L mRNA expression was also obvious in Ramos(EB) and Bjab(EB) cell lines, which had been rendered EBV-positive by the viral infection of parental Ramos and Bjab cells (Fig. 2*C*), suggesting long-term

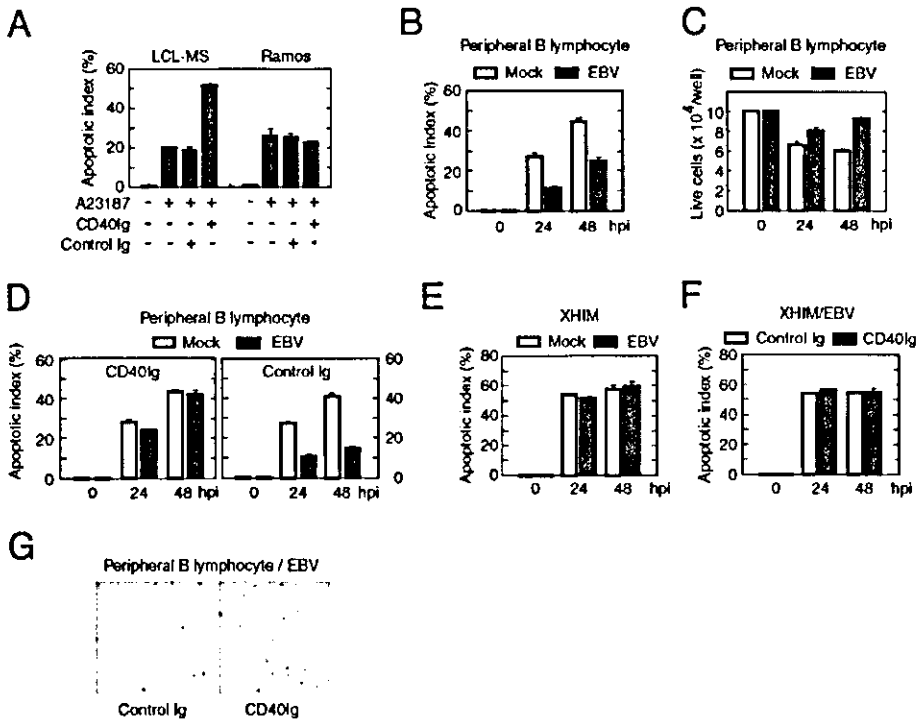

Fig. 3. EBV-induced CD40L inhibits B cell apoptosis. Apoptotic indices are shown as mean values with standard errors from sextuplicate experiments of apoptosis assay. (*A*) Blocking of CD40L with CD40lg (200 μg/ml) up-regulated apoptosis of LCL-MS cells, but not Ramos cells, in the presence of calcium ionophore A23178 (1 μM) for 24 h. (*B*) EBV infection inhibited apoptosis of peripheral B cells. (*C*) Live cell numbers in each culture well of EBV-infected (EBV) or mock-infected peripheral B cells in *B* were counted by standard trypan blue staining. Data represent mean values and standard errors from sextuplicate experiments. (*D*) Blocking of CD40L with CD40lg (200 μg/ml) up-regulated apoptosis of EBV-infected (EBV) peripheral B cells to the level for mock-infected B cells (*Left*). Control Ig did not affect the EBV-mediated inhibition of B cell apoptosis (*Right*). (*E*) EBV-infected and mock-infected XHIM peripheral B cells showed the same level of apoptosis. (*F*) Neither CD40lg (200 μg/ml) nor control Ig influenced apoptosis of EBV-infected XHIM peripheral B cells. (*G*) Apoptotic double-strand breaks of cellular DNA (brown spots) upon EBV infection of peripheral B cells in the presence of CD40lg (200 μg/ml) or control Ig were probed at 24 hpi. (*Left*) Total of 76 cells. (*Right*) Total of 71 cells.

expression of CD40L on EBV-positive B cells (18). Consistently, three of four EBV-positive B cell lines (Raji, Akata, AG876, and P3HR1) derived from Burkitt's lymphomas and two LCLs (LCL-MS and LCL-TM) from normal peripheral B cells expressed CD40L (Fig. 2 *D* and *E*). In addition, when human peripheral B cells were infected with EBV, surface expression of CD40L was induced as early as 24 hpi (Fig. 2*F*). These results indicate that EBV infection of B cells induces ectopic expression of CD40L on their surface.

EBV-Induced CD40L Inhibits B Cell Apoptosis. Encountering antigens through its receptor, B cells need additional signals from their CD40 interacting with CD40L on activated T cells to escape from apoptosis. Thus, we examined whether EBV-induced CD40L inhibits apoptosis of LCL-MS cells and found that blocking of CD40L with CD40Ig, but not the control Ig, up-regulated the Ca^{2+}-induced apoptosis (Fig. 3*A*). In contrast, neither reagent influenced the apoptosis of CD40L-negative Ramos cells, indicating that CD40L plays an antiapoptotic role in the EBV-positive LCL-MS cells. Then, we examined whether this is the case in peripheral blood B cells. Although those B cells underwent apoptosis when cultured *in vitro*, EBV infection inhibited the apoptosis and suppressed the reduction in live cell numbers as early as 24 hpi, followed by a moderate proliferation (Fig. 3 *B* and *C*). However, blocking of CD40L with CD40Ig, but not the control Ig, abrogated the antiapoptotic function of EBV (Fig. 3*D*). Peripheral B cells lacking CD40L from XHIM patients also showed no inhibition of apoptosis, irrespective of CD40Ig, upon EBV infection (Fig. 3 *E* and *F*). In addition, CD40Ig treatment increased normal peripheral B cells carrying double-strand DNA breaks, which are characteristic of apoptotic cells, upon EBV infection (Fig. 3*G*). Together, these results indicate that CD40L induced by EBV infection plays an essential role in the inhibition of host cell apoptosis, thereby facilitating persistent infection of EBV and host cell transformation.

EBV Infection of T Cells Is Associated with Ectopic Expression of CD40. Although EBV is a B lymphotropic agent, its infection of T cells or natural killer cells is seen in patients with T cell or natural killer cell type CAEBV, which is often associated with clonal expansion of the infected cells and consequent malignancies (1, 19). Interestingly, ectopic expression of CD40 was found in EBV-positive T cell lines (SKN-P, SIS) derived from T cell type CAEBV patients (Fig. 4 *A* and *B*) (20). Furthermore, we found that a fraction of the peripheral T cells of T cell type CAEBV patients expressed CD40 on their surface (Fig. 4*C*), whereas those of healthy donors were negative for it (data not shown). Because a majority of T cells are not infected with EBV even in T cell type CAEBV patients (1, 19), we further divided those peripheral T cells into CD40-negative or CD40-enriched fractions and found that the latter T cells have a high viral load (Fig. 4 *C* and *D*). In contrast, T cells of the CD40-negative fraction showed undetectable levels of EBV DNA, demonstrating a tight link between EBV infection and ectopic expression of CD40 on peripheral T cells. In addition, T cells of the CD40-enriched fraction, but not of the CD40-negative one, showed up-regulation of Ca^{2+}-induced apoptosis in the presence of CD40Ig (Fig. 4*D*). These results suggest that EBV infection induces the expression of functional CD40 on peripheral T cells, which may contribute to the clonal expansion of host cells and consequent malignancies of CAEBV patients. To test directly whether EBV infection induces CD40 expression on T cells, we studied Jurkat T cells upon EBV infection and found that it did in terms of mRNA and surface protein expression. (Fig. 4 *E* and *F*). EBV with a UV-inactivated genome induced neither CD40 nor EBNA1, indicating that viral gene expression is required for CD40 expression (Fig. 4*E*).

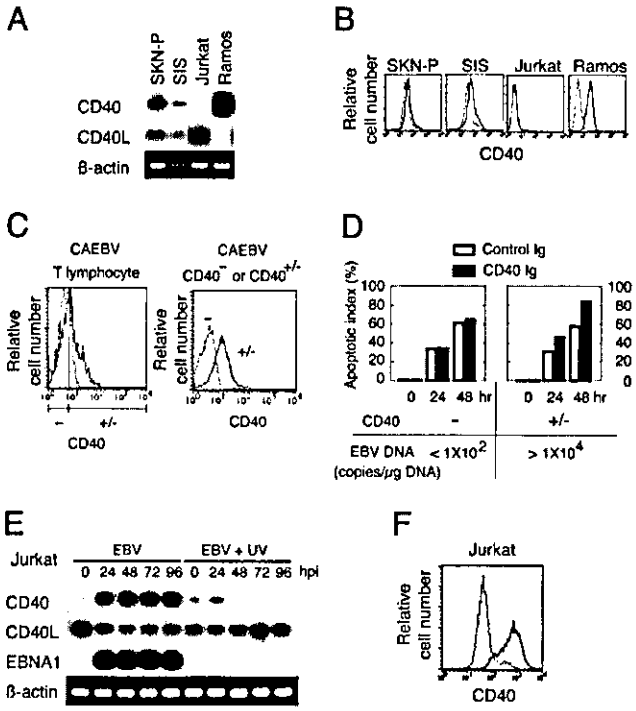

Fig. 4. EBV infection of T cells is associated with ectopic expression of CD40. (*A*) Expression of the indicated mRNA in the EBV-positive T cells (SKN-P and SIS) and the EBV-negative T (Jurkat) and B (Ramos) cells was examined as described in Fig. 2*A*. (*B*) Surface expression of CD40 was examined by flow cytometry with mAb to CD40 (solid line) or isotype-matched control Ig (dotted line). (*C*) Flow cytometry with mAb to CD40 (solid line, *Left*) shows its surface expression on a fraction of peripheral T cells of CAEBV patients. Isotype-matched Ig was used for control (dotted line, *Left*). These CAEBV T cells were sorted into CD40-negative (−) and CD40-enriched (±) fractions, which were monitored by additional flow cytometry (*Right*). (*D*) Peripheral T cells of the CD40-enriched fraction (±) prepared in *C* contained high copy numbers of EBV DNA and showed up-regulation of apoptosis with CD40Ig (200 μg/ml) in the presence of Ca^{2+} ionophore A23178 (1 μM) for the indicated periods (*Right*). Peripheral T cells of the CD40-negative fraction (−) contained undetectable levels of EBV DNA, and their apoptosis was insensitive to CD40Ig (*Left*). Apoptotic indices are shown as mean values with standard errors from sextuplicate experiments of apoptosis assay. (*E*) EBV infection induces CD40 mRNA expression in Jurkat T cells. Expression of the indicated mRNA in EBV-infected Jurkat T cells at the indicated hpi was examined as described in Fig. 2*A* (EBV). EBV with an UV-inactivated genome induced neither CD40 nor EBNA1 mRNA (EBV+UV). (*F*) Flow cytometry with mAb to CD40 shows its surface expression on EBV-infected (solid line), but not mock-infected (dotted line), Jurkat T cells at 48 hpi.

Implications. It is widely accepted that LMP1 plays an essential role in B cell activation and transformation by triggering an intracellular signaling cascade similar to that downstream of CD40, which recruits the TRAF family of signal mediators (1, 4, 6, 21, 22). For example, both LMP1 and CD40 recruit TRAF2, TRAF3, and TRAF5 to induce activation of c-Jun N-terminal kinase and NF-κB. However, as reported here, CD40L/CD40 signaling is still required for the antiapoptotic function of EBV and B cell transformation even in the presence of LMP1 upon EBV infection. There are reports that LMP1 cannot fully compensate for a deficiency of CD40 in mice and that LMP1 and CD40 do not interact with exactly the same sets of signaling molecules, indicating that their signaling pathways differ in some respects (6, 22, 23). Thus, we propose that EBV-induced CD40L/CD40 signaling cooperates with LMP1 in B cell survival and transformation, as they can cooperate for B cell activation (24). On the other hand, it is noteworthy that several autoimmune diseases, such as systemic lupus erythematosus, are asso-

ciated with EBV infection and the ectopic expression of CD40L on B cells (25, 26). Because transgenic mice expressing CD40L on their B cells display symptoms of lupus-like disease, EBV-induced CD40L may be one of the etiologic agents for such human autoimmune diseases (27).

We have demonstrated that EBV infection of B cells induces expression of CD40L as a crucial effector in host cell survival and transformation and that EBV infection of T cells is associated with ectopic expression of CD40 in CAEBV patients. It was recently shown that constitutive expression of CD40L on B cells can stimulate CD40-mediated growth signals (4, 27–30), suggesting that EBV-induced CD40L facilitates B cell proliferation as well. The CD40L expression on LCLs and the other EBV-positive B cell lines suggests long-term expression of EBV-induced CD40L. Therefore, CD40L might play a role not only in the establishment but also in the maintenance of persistent infection of EBV, which would last for a lifetime, and it might contribute to B cell malignancies or other EBV-associated diseases during this period. Understanding how CD40L/CD40 signaling is induced and works on EBV infection of lymphocytes may provide a novel therapeutic target.

We thank H. Nishikawa and Y. Zhu for flow cytometry; M. R. Kehry for CD40Ig; S. Imai and T. Sairenji for lymphoid cell lines; E. Kieff for S12 mAb; F. Mizuno for antiserum to EBNA; M. Kondo for valuable support; H. Kikutani, T. Morio, K. Nakajima, T. Yamamoto, D. Baltimore, S. Fujiwara, K. Hirai, and the other members of our laboratories for helpful discussions; and T. Tsubata, O. Higuchi, and T. Yasuda for critically reading the manuscript. This work was supported by Grants-in-Aid for Scientific Research on Priority Areas from the Ministry of Education, Culture, Sports, Science, and Technology of Japan.

1. Rickinson, A. B. & Kieff, E. (2001) in *Fields Virology*, eds. Knipe, D. M. & Howley, P. M. (Lippincott, Philadelphia), Vol. 2, pp. 2575–2627.
2. Kulwichit, W., Edwards, R. H., Davenport, E. M., Baskar, J. F., Godfrey, V. & Raab-Traub, N. (1998) *Proc. Natl. Acad. Sci. USA* **95,** 11963–11968.
3. Zimber-Strobl, U., Kempkes, B., Marschall, G., Zeidler, R., Van Kooten, C., Banchereau, J., Bornkamm, G. W. & Hammerschmidt, W. (1996) *EMBO J.* **15,** 7070–7078.
4. Schonbeck, U. & Libby, P. (2001) *Cell. Mol. Life Sci.* **58,** 4–43.
5. Callard, R. E., Armitage, R. J., Fanslow, W. C. & Spriggs, M. K. (1993) *Immunol. Today* **14,** 559–564.
6. Lam, N. & Sugden, B. (2002) *Cell. Signalling* **15,** 9–16.
7. Mann, K. P., Staunton, D. & Thorley-Lawson, D. A. (1985) *J. Virol.* **55,** 710–720.
8. Wang, F., Gregory, C., Sample, C., Rowe, M., Liebowitz, D., Murray, R., Rickinson, A. & Kieff, E. (1990) *J. Virol.* **64,** 2309–2318.
9. Rousset, F., Garcia, E., Defrance, T., Peronne, C., Vezzio, N., Hsu, D. H., Kastelein, R., Moore, K. W. & Banchereau, J. (1992) *Proc. Natl. Acad. Sci. USA* **89,** 1890–1893.
10. Sinclair, A. J., Palmero, I., Peters, G. & Farrell, P. J. (1994) *EMBO J.* **13,** 3321–3328.
11. Reedman, B. M. & Klein, G. (1973) *Int. J. Cancer* **11,** 499–520.
12. Chen, C. L., Sadler, R. H., Walling, D. M., Su, I. J., Hsieh, H. C. & Raab-Traub, N. (1993) *J. Virol.* **67,** 6303–6308.
13. Duke, R. C. & Cohen, J. P. (1994) in *Current Protocols in Immunology*, eds. Coligan, J. E., Kruisbeek, A. M., Margulies, D. H., Shevach, E. M. & Strober, W. (Wiley, New York), Unit 3.17, pp. 1–8.
14. Emig, M., Saussele, S., Wittor, H., Weisser, A., Reiter, A., Willer, A., Berger, U., Hehlmann, R., Cross, N. C. & Hochhaus, A. (1999) *Leukemia* **13,** 1825–1832.
15. Castle, B. E., Kishimoto, K., Stearns, C., Brown, M. L. & Kehry, M. R. (1993) *J. Immunol.* **151,** 1777–1788.
16. Levy, J., Espanol-Boren, T., Thomas, C., Fischer, A., Tovo, P., Bordigoni, P., Resnick, I., Fasth, A., Baer, M., Gomez, L., *et al.* (1997) *J. Pediatr.* **131,** 47–54.
17. Okano, M. & Gross, T. G. (2000) *Am. J. Med. Sci.* **319,** 392–396.
18. Fresen, K. O. & Hausen, H. (1976) *Int. J. Cancer* **17,** 161–166.
19. Kimura, H., Hoshino, Y., Kanegane, H., Tsuge, I., Okamura, T., Kawa, K. & Morishima, T. (2001) *Blood* **98,** 280–286.
20. Imai, S., Sugiura, M., Oikawa, O., Koizumi, S., Hirao, M., Kimura, H., Hayashibara, H., Terai, N., Tsutsumi, H., Oda, T., *et al.* (1996) *Blood* **87,** 1446–1457.
21. Mosialos, G., Birkenbach, M., Yalamanchili, R., VanArsdale, T., Ware, C. & Kieff, E. (1995) *Cell* **80,** 389–399.
22. Thorley-Lawson, D. A. (2001) *Nat. Rev. Immunol.* **1,** 75–82.
23. Uchida, J., Yasui, T., Takaoka-Shichijo, Y., Muraoka, M., Kulwichit, W., Raab-Traub, N. & Kikutani, H. (1999) *Science* **286,** 300–303.
24. Busch, L. K. & Bishop, G. A. (1999) *J. Immunol.* **162,** 2555–2561.
25. James, J. A., Neas, B. R., Moser, K. L., Hall, T., Bruner, G. R., Sestak, A. L. & Harley, J. B. (2001) *Arthritis Rheum.* **44,** 1122–1126.
26. Datta, S. K. & Kalled, S. L. (1997) *Arthritis Rheum.* **40,** 1735–1745.
27. Higuchi, T., Aiba, Y., Nomura, T., Matsuda, J., Mochida, K., Suzuki, M., Kikutani, H., Honjo, T., Nishioka, K. & Tsubata, T. (2002) *J. Immunol.* **168,** 9–12.
28. Pham, L. V., Tamayo, A. T., Yoshimura, L. C., Lo, P., Terry, N., Reid, P. S. & Ford, R. J. (2002) *Immunity* **16,** 37–50.
29. Grammer, A. C., Bergman, M. C., Miura, Y., Fujita, K., Davis, L. S. & Lipsky, P. E. (1995) *J. Immunol.* **154,** 4996–5010.
30. Kehry, M. R. (1996) *J. Immunol.* **156,** 2345–2348.

American Journal of Hematology 76:33–39 (2004)

Allogeneic Hematopoietic Stem Cell Transplantation for Seven Children With X-Linked Hyper-IgM Syndrome: A Single Center Experience

Daisuke Tomizawa, Kohsuke Imai, Sukeyuki Ito, Michiko Kajiwara, Yoshiyuki Minegishi, Masayuki Nagasawa,* Tomohiro Morio, Shigeaki Nonoyama, and Shuki Mizutani

Department of Pediatrics and Developmental Biology, Graduate School, Tokyo Medical and Dental University, Tokyo, Japan

X-linked hyper-IgM syndrome (XHIM), or hyper-IgM syndrome type 1 (HIGM1), is a rare primary immunodeficiency disorder susceptible to recurrent bacterial infection and opportunistic infection such as *Pneumocystis carinii* and *Cryptosporidium parvum*. The long-term outcome is quite poor, and allogeneic hematopoietic stem cell transplantation (HSCT) offers the only cure. Seven patients with XHIM, from age 3 to 19 years (mean 11.3 years), underwent allogeneic HSCT in our institution. Details of pre- and post-transplantation data and transplantation procedure were analyzed retrospectively. The donors were HLA-identical siblings for three patients and HLA-identical unrelated donors for four patients. All but one received conventional conditioning regimen consisting of busulfan and cyclophosphamide and prophylaxis for graft-versus-host disease (GVHD) consisting of cyclosporine and methotrexate. Five out of seven patients are alive and well with normal CD40L expression, and four of these five are free of intravenous immunoglobulin supplementation. The two patients who died had prolonged episodes of severe and recurrent infections and organ damage. We conclude that conventional allogeneic HSCT from HLA matched related or unrelated donors is curative and feasible for XHIM patients, if performed before significant infections and organ damage occur. For the high-risk patients, an alternative approach including nonmyeloablative HSCT may be more feasible. Am. J. Hematol. 76:33–39, 2004. © 2004 Wiley-Liss, Inc.

Key words: X-linked hyper-IgM syndrome; CD40 ligand; hematopoietic stem cell transplantation

INTRODUCTION

X-linked hyper-IgM syndrome (XHIM), also known as hyper-IgM syndrome type 1 (HIGM1), is a rare genetic disorder characterized by defective B-cell immunoglobulin isotype switching, which results in markedly decreased serum levels of IgG and IgA and elevated or normal levels of IgM [1]. The disease is caused by defective expression of the CD40 ligand (CD40L) on the surface of activated T cells [2–5]. Interaction of CD40L with CD40 on both B cells and monocyte derived cells is critical for immunoglobulin isotype switching as well as for activation of macrophages and functional differentiation of T cells [6]. The molecular defect is caused by mutations in the gene encoding for CD40L (CD154), located at Xq26.3-27. Point mutations, insertions, deletions, or splice-site mutations of the *CD40L* gene have been described in patients with XHIM [7,8].

Clinically, patients with the disorder have serious and recurrent pyogenic infections caused by encapsulated bacteria. They are also susceptible to infections with opportunistic microorganisms such as *Pneumocystis carinii, Cryptosporidium parvum*, and *Histo-*

*Correspondence to: Masayuki Nagasawa, M.D., PhD., Department of Pediatrics and Developmental Biology, Graduate School, Tokyo Medical and Dental University, 1-5-45, Yushima, Bunkyo-ku, Tokyo, 113-8519, Japan. E-mail: mnagasawa.ped@tmd.ac.jp

Received for publication 5 August 2003; Accepted 19 December 2003

Published online in Wiley InterScience (www.interscience.wiley.com). DOI: 10.1002/ajh.20044

plasma capsulatum. *C. parvum* causes unremitting diarrhea and is associated with sclerosing cholangitis, cirrhosis, and liver cancer [9]. Other complications include neutropenia, autoimmune disease, and lymphomas. It is estimated that only 20% of the patients will reach their third decade of life and that 75% of these patients will have liver complications [10].

Prophylactic co-trimoxazole and intravenous immunoglobulin replacement are the mainstays of supportive treatment, together with advice to taking boiled water to prevent cryptosporidial infection. Granulocyte colony stimulating factor (G-CSF) can improve neutropenia. Since XHIM is considered as a combined immunodeficiency disorder, characterized not only by humoral but also by cellular immune defects, only hematopoietic stem cell transplantation (HSCT) can cure the genetic defect and offers a chance for long-term survival. However, HSCT for immunodeficiency disease is not without risk. Older age, ongoing serious infections, lung or liver diseases, and lack of availability of a well-matched donor are associated with poor outcome after HSCT as previously mentioned for the other primary immunodeficiency disorders such as the Wiskott–Aldrich syndrome [11].

There have been several further successful reports of allogeneic HSCT for XHIM patients, but most of them are single case reports because of the rarity of the disease [12–24]. We report here the experience of HSCT for seven cases with XHIM in a single institution, which is the largest ever reported in Japan.

PATIENTS AND METHODS

This retrospective study involved seven patients with XHIM who received allogeneic HSCT in our institution between December 1998 and September 2002, with a follow-up period of between 0.9 and 4.2 years. Written informed consent to the transplantation was obtained from the parents of each patient.

The diagnosis of XHIM was confirmed by demonstrating the absence of CD40L on mononuclear cells separated on Ficoll, stimulated for 4 hr with phorbol myristate acetate, 20 ng/mL, and then ionomycin, 1,000 ng/mL, and stained with CD3 and CD40L monoclonal antibodies, as described before [25]. Mutations in the *CD40L* gene were also demonstrated by single-strand conformation polymorphism analysis of individual exons of the *CD40L* gene and sequence of affected exon [26].

Before transplantation, all patients were assessed as to clinical status and complications including pre-existing infections. Other information included details of the transplant procedure; particularly donor type and HLA match, conditioning regimens, and prophylaxis for acute graft-versus-host disease (GVHD). The post-transplantation data were recorded including description of infective episodes, engraftment details, complications, and outcome.

Immunological recovery of T and B lymphocytes after transplantation was assessed by CD40L expression on mononuclear cells as mentioned before, and by other standard methods (T-cell and B-cell markers, in vitro T-cell proliferation induced by lectin, serum immunoglobulin concentrations, and serum antibodies after immunization). We also measured serum levels of soluble CD40L (sCD40L), which is undetectable in XHIM patients, by enzyme-linked immunosorbent assay (ELISA kit from Bender MedSystems, Austria) in selected patients (patients 3, 4, and 5) [27].

RESULTS

Pre-transplant Characteristics of Patients

All seven boys had defective CD40L expression on activated T lymphocytes and mutations in the *CD40L* gene (Table I). Patient 4 and Patient 6 are siblings.

Five boys previously had *P. carinii* pneumonitis (Table II). Patient 2 had bronchiectasis and chronic bronchitis with impaired pulmonary function. Patient 5 had lung epithelioid granuloma, which was resected under thoracoscopy before transplantation. Pathologically, *P. carinii* was detected in the granuloma.

Patient 1 had documented cryptosporidial infection with severe diarrhea and malnutrition, which led to failure to thrive since he was 11 years old. The patient also had cryptococcosis and sclerosing cholangitis. None had liver cirrhosis or hepatocellular carcinoma. There were no cases of cytomegalovirus infection. Three patients required G-CSF before transplantation because of severe neutropenia. All seven patients received periodical intravenous immunoglobulin replacement and prophylactic co-trimoxazole. Patient 2 had angioma-like eruptions on his body trunk, and skin biopsy revealed Kaposi's sarcoma. Interestingly, the eruptions disappeared during and after conditioning chemotherapy.

TABLE I. Mutations of the *CD40L* Gene of the Patients

Patient no.	*CD40L* gene analysis
1	Deletion; 198C at exon 5
2	Missense mutation; T713C (Leu231Ser) at exon 5
3	Missense mutation; G697A (Gly226Arg) at exon 5
4	Deletion; 178-181 (ATAG) at exon 2
5	Nonsense mutation; G441A (Try140Stop) at exon 5
6	Deletion; 178–181 (ATAG) at exon 2
7	Deletion; 177G at exon 1

TABLE II. Pre-transplantation Status of the Patients

Patient no.	Age at diagnosis	Previous PCP[a]	Other lung complications	*C. parvum* infection	Neutropenia	Others
1	14 years	+	–	+	–	Failure to thrive, osteoporosis, sclerosing cholangitis, cryptococcosis
2	8 months	+	Bronchiectasis	–	+	Kaposi's sarcoma
3	2 years	–	Pneumonia	–	+	Otitis media
4	4 months	+	–	–	–	—
5	11 months	+	Epithelioid granuloma[b]	–	–	—
6	3 months	–	–	–	–	Sinusitis
7	10 months	+	–	–	+	Sinusitis

[a]PCP, *Pneumocystis carinii* pneumonia.
[b]*P. carinii*-related.

Hematopoietic Stem Cell Transplantation

Age at HSCT ranged from 3 to 19 years (mean 11.3 years) (Table III). Three patients received bone marrow or peripheral blood stem cells from HLA identical sibling donors, and the other four received marrow from HLA matched unrelated donors. As for a conditioning regimen, six patients received busulphan 4 mg/kg p.o. in divided doses daily for four consecutive days (total dose 16 mg/kg) and cyclophosphamide 50 mg/kg once daily i.v. for four consecutive days (total dose 200 mg/kg). Patient 1 received total body irradiation (total 12 Gy, hyperfractionated) and cyclophosphamide 60 mg/kg i.v. daily for two consecutive days (total dose 120 mg/kg).

Six patients received cyclosporine and short-term methotrexate for acute GVHD prophylaxis, and Patient 1 received only cyclosporine due to severe pre-transplant infectious status. None was T-cell depleted or CD34-positive stem cell selected.

Post-transplant Courses

Five of the seven patients had evidence of full engraftment after transplantation and the remaining two (Patient 1 and Patient 2) showed only neutrophil engraftment and were never free of platelet transfusion (Table IV). All five patients with full engraftment are alive and well with normal CD40L expression. Immunological recovery was analyzed for the three patients (Patients 3, 4, and 5) whose observation time was more than three years after transplantation (Table V). All three patients are free of intravenous immunoglobulin supplementation and have made adequate serological responses to attenuated vaccination such as pertussis and later to live vaccination such as measles. Elevation of sCD40L serum levels, which could not be detected before transplantation, was also observed in all these patients (Fig. 1). On the other hand, Patient 6 and Patient 7, who received HSCT the latest with observation period of only 1.5 years and 0.9 year, respectively, are still receiving immunosuppressive therapy because of chronic GVHD of skin. Patient 6 is free of intravenous immunoglobulin supplementation for more than 11 months, but Patient 7 still needs supplementation.

Two patients (Patient 4 and Patient 5), both with episodes of previous *P. carinii* infection, had reactivation of *P. carinii* pneumonitis and were successfully treated by increasing dose of sulfamethoxazole–trimethoprim. No other infectious episodes were seen among surviving patients, except one patient (Patient 4)

TABLE III. Transplantation Data of the Patients*

Patient no.	Age at transplant	Type of transplant	Conditioning regimen	Nucleated cells/kg	$CD34^+$ cells/kg	GVHD prophylaxis
1	17 years	HLA-id sibling/PBSC	TBI/CY	NA	9.00×10^6	CsA
2	15 years	HLA-id URD/BM	BU/CY	4.76×10^8	5.08×10^6	CsA/MTX
3	4 years	HLA-id URD/BM	BU/CY	3.32×10^8	4.80×10^6	CsA/MTX
4	3 years	HLA-id URD/BM	BU/CY	4.85×10^8	2.00×10^6	CsA/MTX
5	18 years	HLA-id sibling/BM	BU/CY	3.83×10^8	NA	CsA/MTX
6	3 years	HLA-id URD/BM	BU/CY	6.52×10^8	2.35×10^6	CsA/MTX
7	19 years	HLA-id sibling/BM	BU/CY	1.96×10^8	8.72×10^6	CsA/MTX

*Abbreviations: HLA-id sibling, HLA identical sibling; HLA-id URD, HLA identical unrelated donor; PBSC, peripheral blood derived stem cells; BM, bone marrow; TBI, total body irradiation (12 Gy); BU, busulphan (16 mg/kg); CY, cyclophosphamide (200 mg/kg or 120 mg/kg for Patient 1); GVHD, graft-versus-host disease; CsA, cyclosporine; MTX, methotrexate; NA, not available.

TABLE IV. Post-transplantation Patient Data*

Patient no.	Neutrophil engraftment[a] (day)	Last platelet transfusion (day)	aGVHD	cGVHD	Infection	Other complications	Outcome (years post HSCT)
1	8	—	—	—	Cryptosporidiosis, sepsis	Renal failure, secondary graft failure	Dead (+63 days); DIC, MOF
2	16	—	Grade 4	—	Bronchopneumonia, *Candida* enteritis, pulmonary aspergillosis	VOD, secondary graft failure	Dead (+89 days); ARDS, pulmonary aspergillosis
3	14	51	...	—	—	—	Alive (+4.2)
4	14	100	Grade 2	—	*C. difficile* enteritis	—	Alive (+3.3)
5	12	34	Grade 2	—	PCP	TMA, pneumothorax	Alive (+3.1)
6	14	20	Grade 2	Skin	PCP	—	Alive (+1.5)
7	14	42	—	Skin, oral	—	TMA	Alive (+0.9)

*Abbreviations: aGVHD, acute graft-versus-host disease; cGVHD, chronic graft-versus-host disease; PCP, *Pneumocystis carinii* pneumonia; VOD, Veno-occlusive disease; TMA, thrombotic microangiopathy; HSCT, hematopoietic stem cell transplantation; DIC, disseminated intravascular coagulopathy; MOF, multiple organ failure; ARDS, acute respiratory distress syndrome.
[a]Neutrophil engraftment: the first of three consecutive days on which the patient's absolute neutrophil count was above 500 per cubic millimeter.
[b]Platelet independence: the day of the last platelet transfusion.

TABLE V. Immunological Recovery of Selected Survived Patients After HSCT*

Patient no.	CD40L expression	In vitro T-cell proliferation	Serum immunoglobulin (mg/dL) at diagnosis/post-SCT			IVIG independence	Immunization
			IgM	IgG	IgA		
3	+	+	592/367	12/1093	2/103	+	+
4	+	+	93/152	73/1421	<31/93	+	+
5	+	+	377/174	292/844	68/163	+	+

*Abbreviations: CD40L, CD40 ligand; IVIG, intravenous immunoglobulin supplementation; immunization, immunization with vaccines.

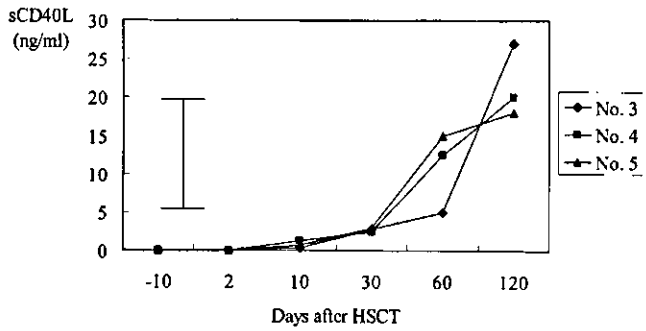

Fig. 1. Serum levels of soluble CD40 ligand after transplantation. Error bar indicates normal values (mean ± SD). Abbreviations: sCD40L, soluble CD40 ligand; HSCT, hematopoietic stem cell transplantation.

suffered from *Clostridium difficile* enteritis. Acute GVHD was seen in four patients: Patient 2 developed grade 4 GVHD (described later in detail), and Patients 4, 5, and 6 developed grade 2 GVHD presenting with fever and skin involvement, which resolved immediately with administration of corticosteroid and administration of tacrolimus in one patient (Patient 6). Two patients (Patient 6 and Patient 7) developed chronic GVHD, which was well controlled by immunosuppressive therapy with corticosteroid and cyclosporine. Two patients (Patient 5 and Patient 7) developed thrombocytopenia and Coombs' test-negative hemolytic anemia, which was diagnosed as thrombotic microangiopathy. These resolved after reducing cyclosporine dose and administering gabexate mesilate to Patient 5.

Two patients died (Patient 1 and Patient 2). Patient 1 was treated with paromomycin, azithromycin, and metronidazole for a prolonged cryptosporidial infection but failed to eliminate before HSCT. Intravenous hyperalimentation improved his nutritional status before HSCT. Peripheral blood stem cells (PBSC) from his HLA-matched sibling were selected for this patient's transplantation in order to establish early engraftment. Although neutrophil engraftment was observed on day +8, a pre-transplant cryptosporidial infection continued to be uncontrollable, refractory to anticryptosporidial therapy. Later he developed sepsis due to *Burkholderia cepacia* and acute renal failure requiring hemodialysis. He also developed graft failure secondary to sepsis on day +22. He received a second PBSC from the same HLA-identical sibling. However, he died from disseminated intravascular coagulopathy and multiorgan failure on day +63.

Patient 2 developed bronchopneumonia due to *Pseudomonas aeruginosa* on day +1 and was successfully treated with antibiotics. He also developed veno-occlusive disease requiring recombinant tissue plasminogen activator on day +7 and grade 2 acute GVHD on day +13, which resolved immediately by corticosteroid therapy. He then developed secondary graft failure, although neutrophil engraftment and full donor chimerism was once confirmed. The cyclosporine dose was reduced to promote the engraftment, but the patient then developed grade 4 GVHD with manifestations of severe maculopapular rash and intractable diarrhea. The GVHD resolved by high-dose methylprednisolone therapy and tacrolimus infusion but was followed by *Candida* enteritis requiring fluconazole administration. He died on day +89 from acute respiratory distress syndrome following severe progressive pulmonary aspergillosis.

DISCUSSION

Long-term prognosis for XHIM patients remains poor despite full supportive treatment with intravenous immunoglobulin replacement therapy, prophylactic co-trimoxazole for *P. carinii* infection, and G-CSF for neutropenia, together with avoiding intake of non-boiled water to prevent cryptosporidial infection, prompt antibacterial treatment, and nutritional support [10]. To date, only immunologic reconstitution by allogeneic HSCT offers a chance of long-term survival, but it is not without risk. Since Fasth reported the first allogeneic HSCT for XHIM, there have been several following reports [12–24]. Although large-scale study is needed to establish evidence for HSCT in this disorder, the rarity of the disease restricted most of them to be single case reports, and the report by Khawaja et al., which included eight cases, is the largest ever published [20]. Our report consists of seven cases;